

SAND86-7028
Unlimited Release
Printed May 1986

Distribution
Category UC-62

An Experimental Investigation of Thermochemical Transport for Solar Applications Using Sulfur Trioxide

J. H. McCrary and Gloria E. McCrary
Physical Science Laboratory
New Mexico State University
Las Cruces, NM 88003

and

Jesus I. Martinez
Solar Distributed Receiver Division
Sandia National Laboratories
Albuquerque, NM 87185

Sandia Contract No. 47-7505

Abstract

The high temperature catalytic dissociation of sulfur trioxide and the synthesis of its products in a closed-loop system presents an attractive prospect for converting, transporting and recovering solar energy. A laboratory scale, closed-loop, sulfur-oxide based experimental system was assembled and operated on the NMSU campus to demonstrate technical feasibility and to study the engineering problems associated with this chemical cycle. The system, which operated at a nominal 500 watts of energy conversion, contained most of the elements of a large scale power plant. Twelve separate experiments were performed with the system in a study of system stability during start-up and shut-down procedures and dissociator temperature variations. Descriptions of the laboratory closed-loop and the chemical reactors are given along with the experimental procedure, conditions, and results for each of the tests. Extensive discussion is given on the solar implications that the results from these experiments may have, and recommendations are made for follow-on experiments that may assist in resolving potential problems for thermochemical transport in a solar-powered plant.

CONTENTS

	<u>page</u>
Abstract	iii
List of Figures	vii
Solar Thermal Technology Foreward	ix
I. Introduction	1
II. Project Objectives	8
III. Experimental Arrangement	9
IV. Experimental Procedure	24
V. Results and Discussion	32
VI. Conclusions and Recommendations	47
VII. References	50
VIII. Appendix	53

LIST OF FIGURES

<u>Fig. No.</u>		<u>Page</u>
1	SO ₃ Dissociation Fraction	6
2	Initial Configuration	10
3	Converter-Heat Exchanger	12
4	Final Configuration	16
5	Thermocouple Locations	20
6	Laboratory Closed Loop System	23
7	Run #12 Power Converted	42
8	SO ₂ Vapor Pressure	54
9	SO ₃ Vapor Pressure	55
10	Teflon Bellows Pump	56
11	Run #1 Dissociator Temperatures	57
12	Run #1 Synthesizer Temperatures	58
13	Run #1 Dissociation Fractions	59
14	Run #2 Dissociator Temperatures	60
15	Run #2 Synthesizer Temperatures	61
16	Run #2 Dissociation Fractions	62
17	Run #3 Dissociator Temperatures	63
18	Run #3 Synthesizer Temperatures	64
19	Run #3 Dissociation Fractions	65
20	Run #5 Dissociator Temperatures	66
21	Run #5 Synthesizer Temperatures	67
22	Run #6 Dissociator Temperatures	68
23	Run #6 Synthesizer Temperatures	69
24	Run #6 Dissociation Fractions	70

LIST OF FIGURES (continued)

<u>Fig. No.</u>		<u>Page</u>
25	Run #7 Dissociator Temperatures	71
26	Run #7 Synthesizer Temperatures	72
27	Run #7 Dissociation Fractions	73
28	Run #8 Dissociator Temperatures	74
29	Run #8 Synthesizer Temperatures	75
30	Run #8 Dissociation Fractions	76
31	Run #9 Dissociator Temperatures	77
32	Run #9 Synthesizer Temperatures	78
33	Run #9 Dissociation Fractions	79
34	Run #10 Dissociator Temperatures	80
35	Run #10 Synthesizer Temperatures	81
36	Run #10 Dissociation Fractions	82
37	Run #11 Dissociator Temperatures	83
38	Run #11 Synthesize Temperatures	84
39	Run #11 Dissociation Fractions	85
40	Run #12 Dissociator Temperatures	86
41	Run #12 Synthesizer Temperatures	87
42	Run #12 Dissociation Fractions	88

SOLAR THERMAL TECHNOLOGY FOREWORD

The research and development described in this document was conducted within the U.S. Department of Energy's (DOE) Solar Thermal Technology Program. The goal of the Solar Thermal Technology Program is to advance the engineering and scientific understanding of solar thermal technology and to establish the technology base from which private industry can develop solar thermal power production options for introduction into the competitive energy market.

Solar thermal technology concentrates solar radiation by means of tracking mirrors or lenses onto a receiver where the solar energy is absorbed as heat and converted into electricity or incorporated into products as process heat. The two primary solar thermal technologies, central receivers and distributed receivers, employ various point and line-focus optics to concentrate sunlight. Current central receiver systems use fields of heliostats (two-axis tracking mirrors) to focus the sun's radiant energy onto a single tower-mounted receiver. Two approaches are predominant for distributed receivers. One approach is to use parabolic dishes up to 17 meters in diameter to track the sun in two axes and use mirrors or Fresnel lenses to focus radiant energy onto a receiver. Another approach is to use troughs and bowls as line-focus tracking reflectors to concentrate sunlight onto receiver tubes along their focal lines. Concentrating collector modules can be used alone or in a multi-module system. The concentrated radiant energy absorbed by the solar thermal receiver is transported to the conversion process by a circulating working fluid. Receiver temperatures range from 100°C in low-temperature troughs to over 1500°C in dish and central receiver systems.

The Solar Thermal Technology Program is directing efforts to advance and improve promising system concepts through the research and development of solar thermal materials, components, and subsystems, and the testing and performance evaluation of subsystems and systems. These efforts are carried out through the technical direction of DOE and its network of national laboratories who work with private industry. Together they have established a comprehensive, goal-directed program to improve performance and provide technically proven options for eventual incorporation into the Nation's energy supply.

To be successful in contributing to an adequate national energy supply at reasonable cost, solar thermal energy must eventually be economically competitive with a variety of other energy sources. Components and system-level performance targets have been developed as quantitative program goals. The performance targets are used in planning research and development activities, measuring progress, assessing alternative technology options, and making optimal component developments. These targets will be pursued vigorously to insure a successful program.

Thermochemical transport is being researched and developed in conjunction with distributed receivers as an alternative to energy transport systems based on sensible or latent heat of heat transfer fluids, with the aim of minimizing heat losses incurred in transport as well as minimizing the insulation requirements for transport lines. A recent comparison of thermochemical and sensible heat transport for a distributed receiver solar field (1) indicated a significant advantage in overall efficiency is realized for an optimized thermochemical system as compared to the overall efficiency of an optimized sensible-heat system. This report documents the results of work performed at the Physical Science Laboratory of New Mexico State University in conjunction with Sandia National Laboratories on a laboratory-scale thermochemical transport loop based on the dissociation of sulfur trioxide.

I. INTRODUCTION:

Because of the diffuse nature of solar energy, its utilization for many processes requires that it be concentrated and very often converted to a more appropriate form of energy. Invariably it becomes necessary to transport the energy to a site that is separate and removed from the collection site. In collecting energy with a field of distributed receivers such as parabolic dishes, the transport of energy becomes a crucial part of the utilization of solar energy and transport losses can have a significant impact on the economic feasibility of this renewable resource. Thermochemical transport (TC-T) has been considered as a means of achieving the transport of converted solar energy with minimal transport losses because of the possibility of achieving the transport at close to ambient temperatures.

TC-T consists of a reversible chemical reaction system in which an endothermic process is carried out at the energy collection site by absorbing thermal energy and converting it to potential chemical energy by dissociating chemical bonds. The dissociated chemicals, preferably gases for ease of transport, are cooled via heat exchangers and transported at close to ambient temperatures to a user site. There the reverse or exothermic process can be carried out releasing the energy associated with bond

formation. The TC-T cycle is completed with the recirculation of the products of the exothermic process back to the energy collection site to repeat the cyclic process.

Several chemical reaction systems have been studied in the past in conjunction with TC-T (2-9) as well as in considering the storage of solar energy (10-12). One of the earliest concepts, proposed by T. A. Chubb (13-18), was Solchem. This concept was based on distributed receivers heated by solar parabolic dishes with thermochemical transport to a central power generating facility. Two chemical reaction systems are presently being investigated experimentally under the Transport and Storage Task of the Distributed Receiver Technology Program at Sandia. The two systems involved are: 1.) the $\text{CO}_2\text{-CH}_4$ reforming-methanation cycle and 2.) the dissociation and synthesis of SO_3 .

An SO_3 based energy conversion and transport loop is uniquely suited to the collection and delivery of high temperature heat energy. The chemical reaction cycle utilizing SO_3 is characterized by simple chemistry and no side reactions. In the presence of a suitable catalyst, SO_3 gas can be dissociated into SO_2 and O_2 at temperatures in the range of 800-1000°C with the endothermic capture of 22.3 kcal. of heat per mole of SO_3 reacted (19). The product gases, after heat exchange, can be transported through pipes at modest temperatures and

pressures to a central thermal storage or power utilization facility. Here, the components of the energy rich mixture of gases can be catalytically recombined at 500-600°C to regenerate the SO₃ and release the chemical heat of reaction. Hence, by passing the gaseous SO₃ through a dissociation reactor in a high temperature receiver, sunlight can be converted into chemical energy in a form which can be readily transported and reconverted to relatively high temperature heat. By using countercurrent heat exchangers in conjunction with the chemical reactors at both ends of the loop, gas circulation piping can be kept at moderate temperatures at which no SO₃ condensation will occur at the working pressure.

Although SO₃ is a highly toxic and potentially corrosive chemical, there are well established rules for handling the material in an industry with production rates of 2×10^{10} kg/yr. In addition, SO₃ is the end product in the atmospheric oxidation of SO₂, a substance introduced into the atmosphere in enormous quantities during the burning of coal. Its use in a closed loop energy conversion and transport process thus imposes no new ecological problems. The use of SO₃ can, however, involve significant materials problems. At 100°C, these problems are not severe, although common material choices are largely restricted to teflon, mild steel, stainless steels, glass, quartz, and ceramics. At receiver temperatures of 1000°C

teflon and steel are not usable. While there are indications that aluminum rich alloys, such as Kanthal A-1, may be usable, the materials of choice for SO₃ energy converters are fused silica, ceramics, and possibly some Incolloys. An effort to address metallic materials compatibility in SO₂/O₂ as well as SO₃ environments was conducted at Sandia by L.J. Weirick (20,21).

Catalyst and materials studies have been previously conducted by the Advanced Energy Systems Division of Westinghouse (22) in Pittsburgh, PA. A Mathey-Bishop catalyst (MB-3), consisting of 1% platinum on alpha alumina, was found to work in SO₃ dissociation/synthesis. Dr. J. F. Pierre generously provided a supply of this MB-3 catalyst for use in this project. In related catalyst aging studies the Rocket Research Company in Redmond, WA found some degradation of a platinum-alumina catalyst during accelerated life aging tests (23).

An experimental investigation of SO₃ dissociation as a method for converting solar energy to chemical heat of reaction was conducted at New Mexico State University in 1979 and 1980 (24,25). During that work an acceptable dissociator/heatexchanger receiver element design was developed. The SO₃ dissociation fraction was measured as a function of space velocity, temperature, and catalyst configuration to help provide a degree of understanding

for optimization of the chemical engineering parameters involved in the design and operation of solar receivers.

Figure 1 represents a typical plot of the SO_3 equilibrium dissociation fraction as a function of temperature for a pressure of 1.6 absolute atmospheres (26). The dissociation fraction is defined as the fraction that the SO_2 concentration constitutes of the sum of the overall concentration of these gases, or

$$\text{D.F.} = [\text{SO}_2] / \{[\text{SO}_2] + [\text{SO}_3]\}$$

From the curve in Figure 1 it is seen that the temperature regions in which the two reactors of a closed-loop system must operate at 1.6 atmospheres are 800-1000°C for the dissociator and 500-650°C for the synthesizer in order to achieve a satisfactory efficiency overall. Different temperatures can be achieved at the synthesizer using different operating pressures as indicated by the dotted curves in Figure 1.

In the present work the sulfur oxide-based energy conversion and transport loop was closed, and the power converted in the dissociator was transported through uninsulated, low temperature lines to a synthesizer reactor where it was recovered as high temperature heat. A small, continuously cycled charge of gas allowed the system to operate continuously for extended periods of time. During seventy-five hours of operation, the only detectable degradation of any system component was a slight discoloration of the dissociation catalyst from a

SO₃ EQUILIBRATION

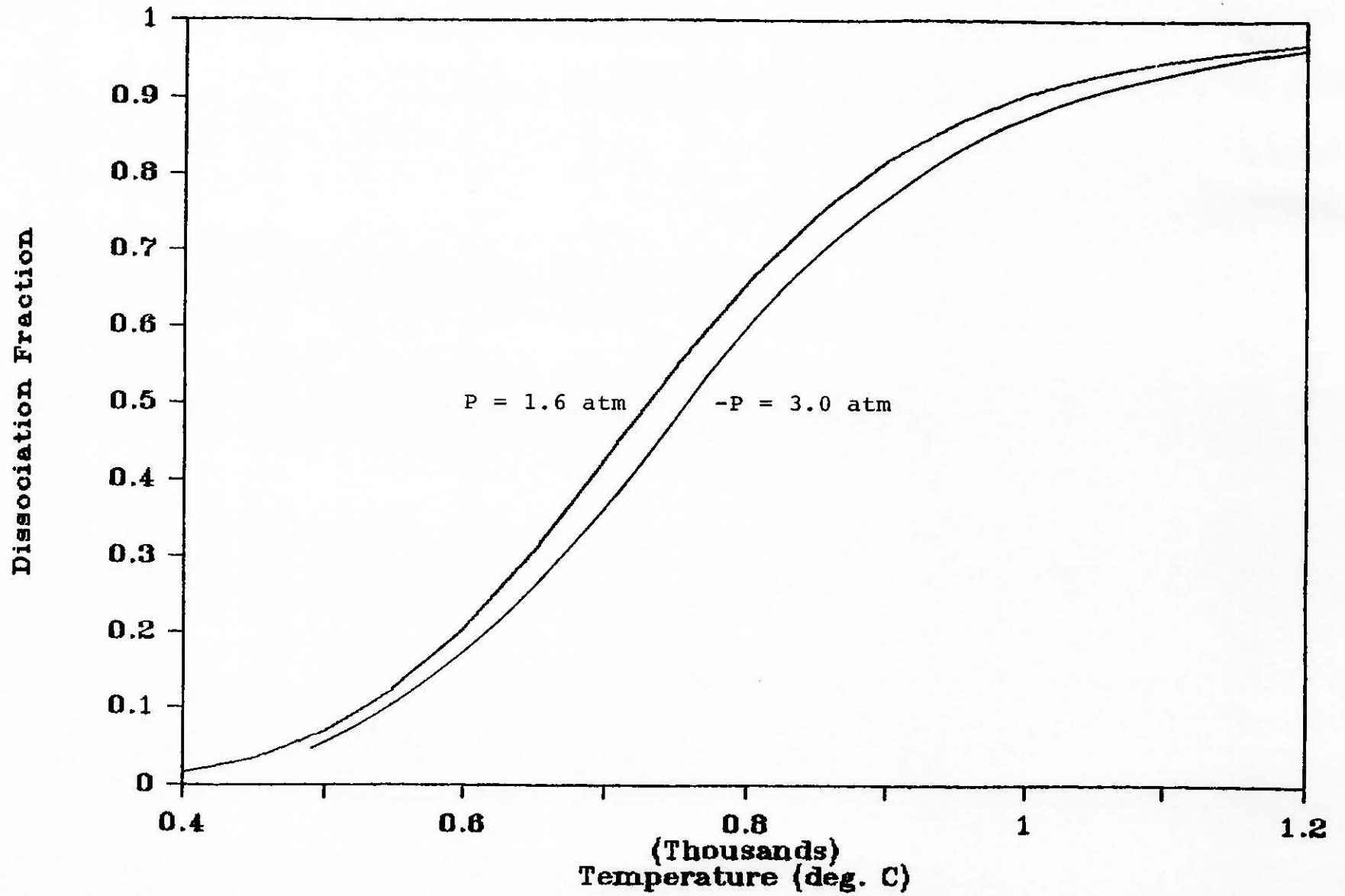


Fig. 1: SO₃ Dissociation Fraction

black to a gray color. It is possible that this discoloration may be associated with a possible loss of platinum from the catalyst surface. Some loss in the reactivity of the dissociator catalyst was evidenced after a high temperature trial during the last experiment.

An estimate of the power converted in a two-reactor, closed-loop system involving sulfur oxide gases can be obtained using the following equation:

$$PC = hm(F_2 - F_1) \quad \text{Eqn. 1}$$

where PC = power converted in kilowatts,

h = heat of reaction = 1.145 kJ/g SO₃ reacted,

m = gas flow rate in g/sec,

F₂ = dissociation fraction in diss. outlet line, and

F₁ = dissociation fraction in dissociator inlet line.

Since volume flow rather than mass flow is measured in these experiments, equation 1 must be amended to account for the difference in the molecular weights of the gases in the two legs of the loop. Thus,

$$PC = 4.1761PV(F_2 - F_1)/(1 + 0.5F_2) \quad \text{Eqn. 2}$$

where P = pressure in the SO₂ line in psia and

V = volume flow rate in the SO₂ line in l/min. at the working pressure.

In equation 2 the gas temperature in the SO₂ line is assumed to be 30°C.

II. Project Objectives:

The principal objective of this task was to perform experimental research on the SO_3 dissociation and recombination processes as these apply to thermochemical energy conversion and transport. The following specific tasks were defined to meet this objective:

1. Design and assemble a laboratory-scale, closed-loop energy conversion, transport, and recovery system based on the high temperature dissociation of gaseous SO_3 and the recombination of its products with the low temperature transport of these gases. Provision shall be made for monitoring and recording temperatures and pressures at selected points in the reactors, heat exchangers, and lines and for measuring and recording the mass flow rate. The molar fraction of the SO_2 in both legs of the loop shall be monitored.
2. Conduct a series of closed-loop experiments to determine the reactivity of the dissociation and recombination reactors and the energy conversion and delivery efficiencies as a function of temperature, pressure, and flow rate.
3. Conduct a series of closed loop experiments to determine whether energy conversion and delivery efficiencies are adversely affected by changes in the length and configuration of the interconnecting tubing between the endothermic and exothermic reactors.

4. Conduct experiments directed toward the definition and resolution of problems associated with system shutdown and start-up after both short and long-term interruptions.
5. After determining the optimum operating parameters of the laboratory-scale, closed-loop system, conduct a series of long-term tests with overnight shut-down simulating the operation of a solar-powered plant.
6. At the optimum operating conditions and after accumulating enough data with only overnight shutdown, conduct a series of long-term tests with periodic interruptions that allow for partial to complete cool down of the reactors and transport system. Determine the effects of these transients on the energy conversion and delivery efficiencies of the system over short and long-term periods.

The degree to which these tasks were completed is discussed in Section VI - Conclusions and Recommendations of this report.

III. Experimental arrangement:

Figure 2 depicts the experimental, closed-loop system as it was originally set up with the synthesizer and dissociator reactors oriented horizontally. The primary components are the two quartz converter/heat exchangers installed with the reactor portions inside of a their respective tube furnaces. The interconnections shown

10

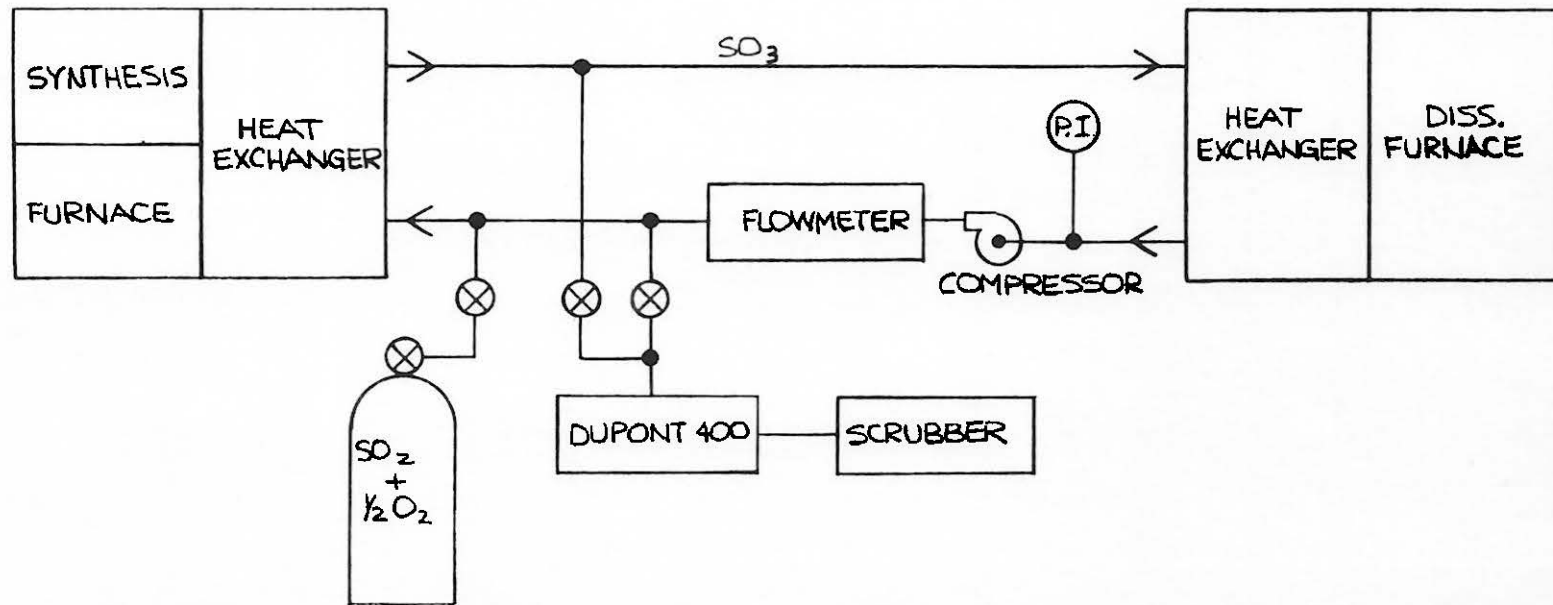


Figure 2: Initial Configuration

consisted of 1/2" teflon tubing with stainless steel fittings. The connection between the quartz tubing of the heat exchangers and the teflon lines consisted of a tight slip fit without any additional clamping. The system was designed to operate with the following nominal specifications:

1. Dissociator temperature	900°C
2. Synthesizer temperature	550°C
3. SO ₃ line temperature	55°C
4. SO ₂ + O ₂ line temperature	30°C
5. Startup feedstock	2SO ₂ + O ₂
6. Volume flow (diss. outlet)	15 l/min.*
7. Pressure (diss. outlet)	1.5 atm. abs.
8. Power converted	500 watts

During the course of the experiment changes to the flow configuration depicted in figure 2 were developed. These will be presented chronologically in the Experimental Procedure section of this report. A description of each of the major system components is presented below.

A. Converter/Heat Exchangers:

The converter/heat exchangers shown in Figure 3 were fabricated from quartz tubing by the William A. Sales Co. of Wheeling, Illinois. The reactor/heat exchangers were purposely designed conservatively in both their reaction capacity and heat exchange capabilities since they were to

*volume flow given at system temperature and pressure

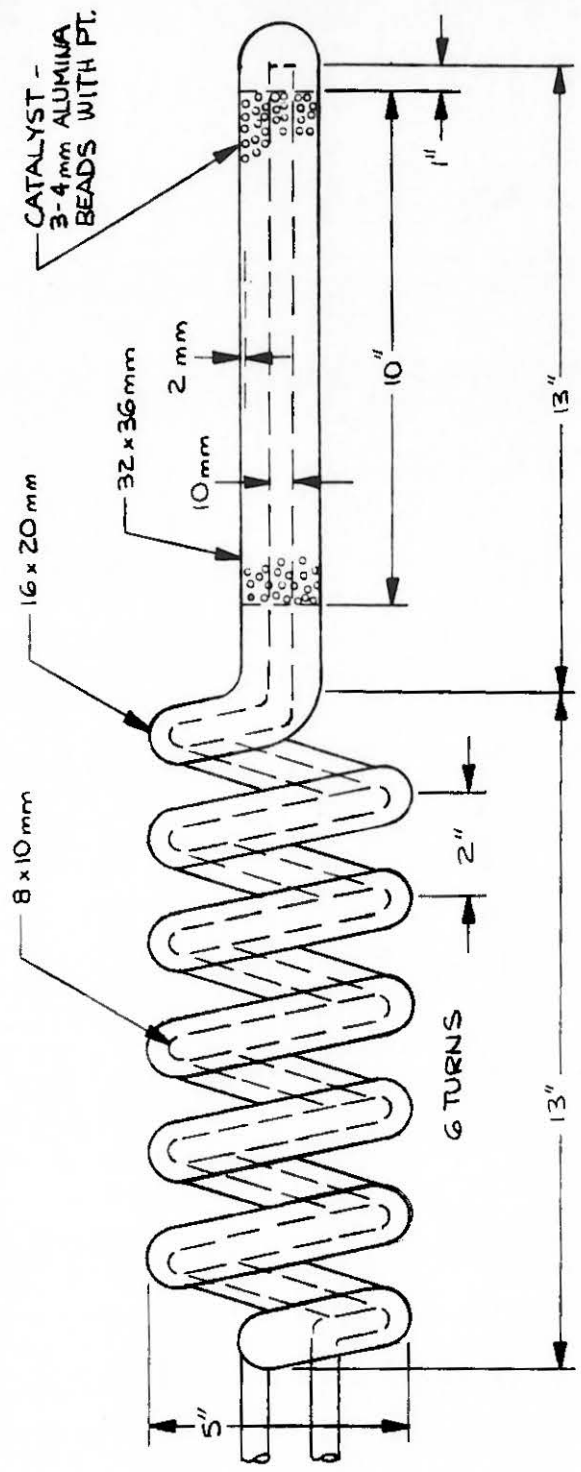


Figure 3: Converter-Heat Exchanger

be used in a research environment and since it was advantageous to use the same vessel in both dissociator and synthesizer furnaces. The reactor volume was calculated to be 184 cm^3 , about one-fourth the volume of the 2-kW JPL reactor tested in earlier experiments (18). This permitted the use of space velocities in the 2000 hr^{-1} to 4000 hr^{-1} range with mass flows of approximately 0.5 g/s. The quartz tubing used in the fabrication of the reactors was capable of withstanding internal pressures of 50 psig.

The catalyst beads were loaded into the reactors by the William A. Sales Co. These contained 0.3% Pt on 4mm diameter alumina spheres obtained from the Engelhard Minerals and Chemical Corp. of Newark, NJ. This catalyst had been purchased several years ago by the Naval Research Laboratory for an earlier related project. This catalyst was found to be unreactive during the first experimental run and consultation with Engelhard scientists revealed that the catalyst support beads contained as much as 12% silica which begins to sinter at 500°C .

The Engelhard catalyst loaded into the reactors was discarded after the first experimental run. Replacement catalyst, manufactured by Mathey-Bishop, Inc. of Malvern, PA, was obtained for this project from Dr. J. F. Pierre of the Advanced Energy Systems of Westinghouse. The catalyst was an MB-3 type consisting of a 1% Pt on 1/8-inch alpha alumina spheres (lot number 269-13-2). Reactor cutting

and resealing was accomplished at the Sandia glass shop with all catalyst handling performed by the principal investigators using lint-free gloves. All subsequent experiments were conducted using this catalyst without any significant problems.

B. Furnaces and Controls:

The reactors were designed to fit into electrically heated, 12-inch long tube furnaces with the heat exchanger portion, packed in high temperature insulation (Carborundum Fiberfrax wool), located just outside the furnace. The dissociator furnace was purchased from Applied Test Systems, Inc. of Butler, PA. Their model 3110 furnace was modified at the factory to include heavy duty windings rated at 2.26 kW and 240 volts.

The synthesizer furnace was of the split shell design to permit easy cooling of the converter tube after the reaction started. This furnace was manufactured by Electro Heat Systems, Inc. in Washington, PA. It was rated at 1.2 kW with 240 volts supplied. Both furnaces were supplied with electrical power from manually controlled variable transformers. The transformer output could be varied from 0 to 240 volts at a maximum current of 26 amperes. During normal system operation the dissociator furnace control ran at about 60% of full output voltage and the synthesizer power input was zero after the initial startup.

C. Lines, Fittings, and Valves:

All lines in the system were made of 12 mm OD by 9.5 mm ID teflon tubing (Cole-Parmer Catalog No. Y6407-40). Teflon fittings were also purchased from the Cole-Parmer company in Chicago, IL. The fittings, which matched the tubing in size, were made so that teflon was the only material which contacted the fluid. Metal nuts and meoprene O-rings compressed the fittings to the tubing. The fittings were specified to have a maximum working pressure of 50 psig. Teflon stopcock type valves were used throughout the system. The valves (Cole-Parmer catalog number 6392-40) had the same nuts and compression rings as the rest of the fittings. The valves had a 4-mm bore. The system, as originally designed, contained three line valves (Figure 2). The number of valves was increased to eight in the final apparatus configuration (Figure 4). The line which carried SO_3 from the synthesizer to the dissociator (top line in both Figures 2 and 4) was heated by an electrical tape to a temperature of about 55°C to prevent condensation of SO_3 in the line (see Figure 9, Appendix).

D. Compressor:

Gas was moved through the system by a two cylinder, all-teflon and glass bellows pump. This pump was purchased from Cole-Parmer Instrument Co. under their catalog number K-7152-60. The pump operated pneumatically and its speed was controlled by adjusting the inlet air pressure.

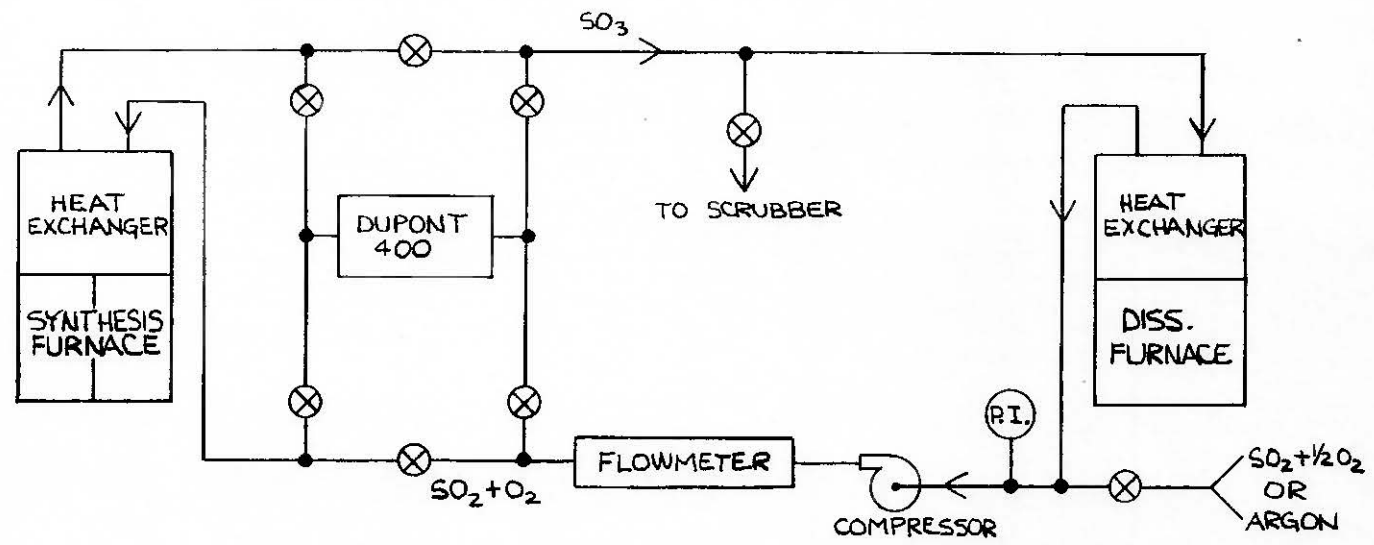


Figure 4: Final Configuration

It had a capacity rating of 0.74 cfm at ambient temperature with a zero pressure differential and 0.52 cfm with a 15 psi differential. The pump was found to be very reliable and relatively easy to clean. Leaks developed around the ends of the glass cylinders, but they were controlled by tightening the clamping nuts. The pumping speed was found to be extremely constant over long periods of time (10 hrs). Figure 10 in the Appendix is a copy of the pump description from the Cole-Parmer catalog. Typical compressor speeds were in the range of 100 to 120 cycles/min.

E. Gas Supply:

It was originally planned that cylinders of pre-mixed SO_2 and O_2 in the ratio of 2 to 1 would supply gas to the closed loop system (see Figure 2). Periodically, gas would be drawn from one line or the other for analysis in the Dupont Model 400 gas analyzer and disposed of through the scrubber. Several problems developed with this mode of operation during the course of the project:

1. A fairly large quantity of gas is needed to obtain an accurate measure of the SO_2 concentration.
2. Because of the SO_2 vapor pressure, cylinders of pre-mixed feedstock could contain only about 50 psi of gas.
3. The supplier of the pre-mixed gas (Liquid Carbonics) decided against further shipment of pre-mixed gases.

4. It was observed that this mode of operation did not constitute a true closed loop.

For these reasons a decision was made to change the system configuration from the one shown in Figure 2 to that of Figure 4. Separate cylinders of SO_2 and O_2 were purchased and a gas proportioner (Matheson model 7372) was used to provide a stoichiometric mixture. This mode of operation proved to be quite successful and also more cost effective in view of the practice of disposal of the analyzed gases through the scrubber.

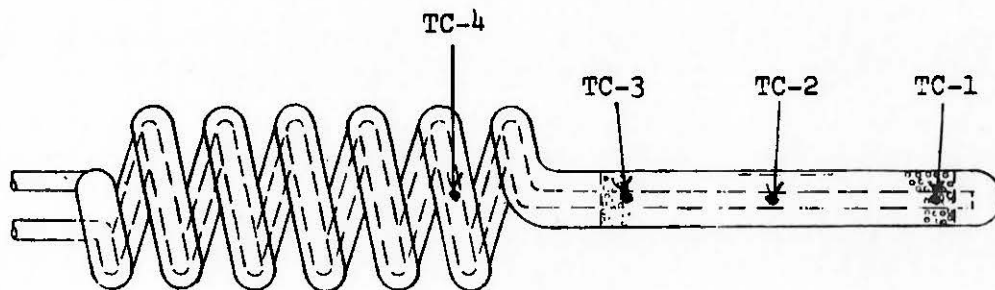
F. Instrumentation:

Gas Analyzer - A Dupont model 400 uv absorption analyzer designed for continuous gas flow was used to measure the SO_2 fraction in both lines of the closed loop system. The optical beam in the instrument is filtered to pass 0.313 micron wavelength radiation which is absorbed by SO_2 but not by SO_3 or O_2 . The sample cell is mounted in an oven whose temperature is controlled at 100°C . The only materials which contact the sample gas are quartz, stainless steel, and teflon. The instrument supplies a 0 to 100 mV analog signal to the data logger. The size of this signal is proportional to the SO_2 volume fraction in two manually selectable ranges; 0 to 70% and 0 to 14%. It was found that the total system flow of 10 to 12 l/min., measured at ambient conditions, could be passed through the Dupont instrument with no perceptible loss of flow rate or pressure. Appropriate use of the

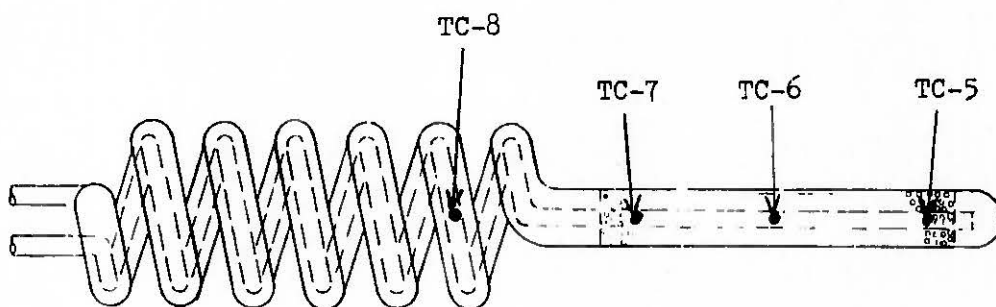
valving shown in Figure 4 permitted the SO_2 concentration to be measured alternately in both legs of the loop.

Thermocouples - Ten type K (chromel-alumel)
thermocouples were used to measure temperatures in the system. The thermocouples were sheathed with 1/16 inch OD stainless steel tubing and were ungrounded. The locations of the first eight thermocouples are shown in Figure 5. These devices were attached to the outside surface of the quartz tubing using a high temperature ceramic cement (Sauereisen) and tied with thermocouple wire. Thermocouples 9 and 10 were mounted on the SO_3 and SO_2 lines, respectively, near the center of their runs. Thermocouple number 11 (copper-constantan) was mounted in the Dupont analyzer oven. All thermocouples were wired directly to the data logger.

Pressure Gauge - A single pressure gauge was located as shown in Figure 4. The device used was a stainless steel Bourdon tube with a 3-inch dial calibrated from 0 to 50 psia. Since the pressure gauge was located at the compressor inlet and the flowmeter at the compressor outlet, a correction had to be applied to the measured pressures before calculating the power converted. Repeated observations made with and without the compressor running indicated a decrease of 10 to 15% in the pressure readings when the compressor was turned on. Since the pressure indicator was installed on the inlet side of the compressor



Synthesizer Reactor



Dissociator Reactor

Figure 5: Thermocouple Locations

(see Figure 2), it is reasonable to assume that the compressor outlet pressure was higher when the compressor was operating. Thus, in calculating power converted, the observed pressures were increased by 10% to correct for the drop across the compressor. The accuracy of pressure readings was estimated at + or - 0.5 psi.

Flowmeter - The volume flowmeter, located as shown in Figure 4, was a 150-mm Aalborg model FM044-40 S rotameter. The unit was calibrated with air at the factory. Aalborg recommended the use of a correction factor equal to the square root of the ratio of the densities of air and feedstock. The rotameter reading was thus multiplied by 0.6 to obtain the volume flow rate of gases in the line. Flowmeter readings were made visually and recorded periodically in the laboratory notebook. Although the rotameter ball oscillated + or - 1 l/min. with the frequency of the compressor, average readings were not difficult to obtain. In our estimation the accuracy of the volume flow rates can be assumed to be + or - 10%.

Data Logger - An Esterline-Angus model PD-2064 data logger was used to record the thermocouple and analyzer signals. This unit can accommodate as many as 31 transducers with any mix of Type K and Type T thermocouples and other analog signals. Thermocouple signals were corrected for cold junction offset and temperatures were recorded in degrees centigrade. The data logger had the capability of recording data as frequently as once every minute or at

slower rates. During most of the experimental runs, which involved either steady state conditions or slow transients, data were recorded at five-minute intervals. The temperature plots presented in the Appendix were obtained from these data.

G. Safety:

Personnel safety must be an important consideration in any system involving toxic substances or potentially hazardous conditions. Safety in these experiments was provided by a fume hood and a gas scrubber.

The fume hood, 7 feet long by 3.5 feet wide by 3 feet high, was fabricated by the PSL machine shop from 0.060-inch stainless steel. A straight, vertical, eight-inch duct led from the top of the hood to a 2-speed, 1400 cfm (free air capacity) blower mounted on the roof of the building. A photograph of the hood with the closed loop system installed is shown in Figure 6.

The SO_2/SO_3 scrubber was constructed after the pattern of Miyamoto (27). It consisted of a 20-inch length of perforated 3/4-inch PVC tubing buried in a sand-lime mixture contained in a 2-foot by 1-foot rectangular box located in the back of the fume hood. This type of scrubber is very efficient in converting SO_2 and SO_3 by reaction with the lime to form calcium sulfite and calcium sulfate, respectively, which remain trapped in the scrubber. This scrubber was used mainly during start-up and

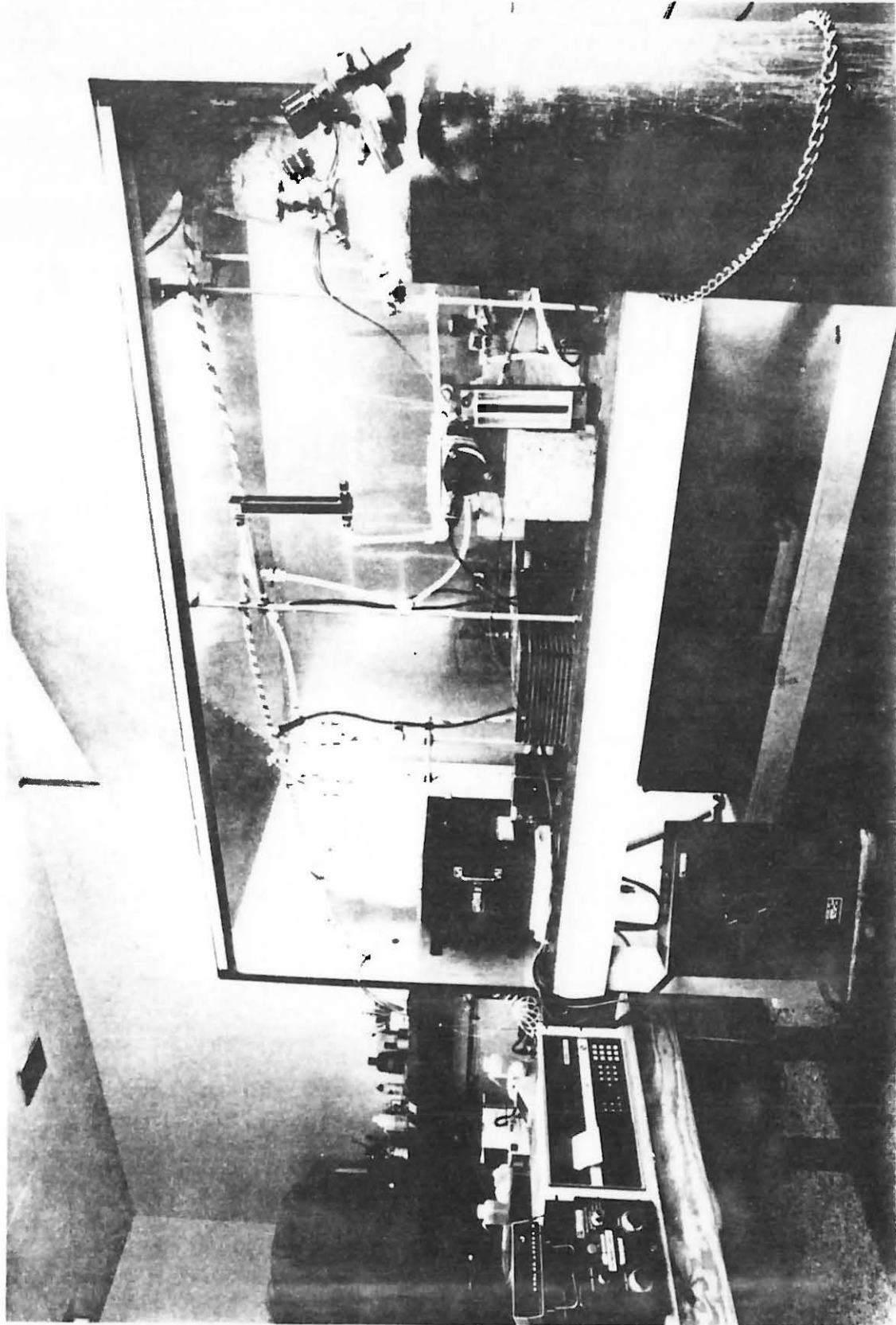


Figure 6: Laboratory Closed-Loop System

shut-down operations to vent small quantities of SO_2 and SO_3 used for flushing or purging the system.

IV. Experimental Procedure:

After the completion of the closed-loop system in accordance with initial plans (Figure 2), a preliminary test (Run #1) was conducted on April 5, 1984. The system was first flushed with argon, the reactors were heated to their operating temperatures, and the system then flushed and filled with the pre-mixed SO_2 and O_2 to a pressure of 15 psia while a flow rate of 8 to 10 l/min (measured at operating conditions) was maintained by the compressor. The system was operated in this mode while repeated analyses were made of gas from both legs of the loop. Gas from both legs exhibited the same dissociation fraction of about 0.25 to 0.30 indicating essentially no dissociation. This composition was commensurate with the temperature of the synthesizer reactor. Run #1 was terminated after 45 minutes.

Efforts to explain the lack of dissociator reactivity eventually pointed to the catalyst. As explained in Section III, the original catalyst loaded was found to be defective and was subsequently replaced with the Mathey-Bishop MB-3 catalyst obtained from the Westinghouse Corp. The catalyst in both reactors was exchanged on April 24, 1984 in the Sandia glass shop. Since the bead size of the replacement catalyst was smaller than that of the original

catalyst, it was necessary to leave about an inch of the old catalyst beads in place in order to contain the new catalyst beads in the reactor. The net effect of this procedure was to shorten the length of the active catalyst bed by about an inch out of a total 9-inch length.

Run #2 was made on May 2, 1984 with the same system configuration as shown in Figure 2. Furnaces were heated with a slow flow of argon in the system. The argon was then flushed out with the pre-mixed feedstock and data were taken at one-minute intervals for 24 minutes. Nominal values of operating parameters during Run #2 were:

dissociator reactor temperature	= 900°C,
synthesizer reactor temperature	= 600°C,
pressure	= 15 psia
flow rate	= 10 l/min.

Energy was successfully converted, transported, and recovered in this run. During the latter half of the run, the dissociation fractions were 0.70 in the dissociator outlet and 0.35 in the synthesizer outlet. These figures correspond to about 175 watts of power converted.

In studying the data from Run #2, catalyst problems were again suspected. Since the catalyst beads were not tightly packed and since the reactors were oriented horizontally, it was suspected that catalyst free channels might exist across the top of the reactor tubes. To eliminate this possibility, both furnace-reactor assemblies were reoriented with their axes vertical. Both

reactors were plumbed so that gas flowed in through the center tube and up through the catalyst bed.

Run #3 was performed on May 10, 1984 with a system configuration as shown in Figure 2 except for the vertical orientation of the reactor-heat exchanger assemblies.

Nominal system parameters were:

dissociator reactor temperature	= 875°C
synthesizer reactor temperature	= 550°C
pressure	= 18 psia
flow rate	= 10 l/min.*

Improved dissociation fractions were noted in this experiment which resulted in a power conversion of 330 watts. The test was terminated after 38 minutes to conserve a dwindling gas supply.

Run #4 was conducted on May 17, 1984 as a demonstration for visiting Sandia personnel. Experimental configuration and operating conditions were identical with those for Run #3. Run #4 was terminated after 22 minutes when the feedstock gas supply was exhausted.

After Run #4 was terminated, the pre-mixed gas input line was removed from the system and replaced with the Matheson gas proportioner operating from separate gas cylinders of SO₂ and O₂. Several preliminary operations were conducted with the furnaces unheated in order to gain experience with the gas proportioner and to check out the gas concentrations calculated from the proportioner

*all flow rates are given at operating conditions

flow rates against the concentrations measured with the Dupont 400 gas analyzer. The concentrations measured with the Dupont analyzer agreed quite well (within about 5%) with the proportioned mixtures.

A decision was made to have Run #5 last for five hours, the first long term experiment. The experimental configuration for Run #5 was still that shown in Figure 2 with the exceptions of a vertical orientation for the reactors and the use of a gas proportioner to supply the feedstock. In order to more closely approximate closed loop operation, Run #5 was made with a minimum of gas analyses. The reason for minimizing the number of gas analyses was to minimize the input of fresh feedstock necessary to replace the analyzed gases exhausted to the scrubber as this cannot be considered a true closed loop. As a consequence, virtually no concentration data were obtained during run #5. With this exception, however, the five-hour run was quite successful. The reactor temperatures were remarkably stable at 900°C and 525°C for the dissociator and synthesizer respectively. Flow rates of 10 to 12 l/min. were maintained at pressures of 15 to 17 psia. Several attempts to measure gas concentrations resulted in loss of pressure before an accurate measurement could be made. Efforts in this direction were thus abandoned. After synthesizer ignition was determined, the synthesizer furnace was turned off and partially opened during the entire five hours.

After Run #5 the system was replumbed as shown in Figure 4 so that all system gas in either leg could be channeled through the Dupont analyzer. Preliminary tests indicated that the flow impedance of the analyzer sample cell was low and could be handled by the compressor. In this mode of operation air was flushed from the system by argon which was then swept out through the scrubber with proportioned SO_2 and O_2 . The system was then pressurized to about 16 psia and sealed off. The result was a true closed loop operation with continuous gas analysis.

Run #6, performed on June 26, was the first test of the new configuration. It was made with operational conditions similar to those attending Run #5:

dissociator reactor temperature	= 900 to 950°C
synthesizer reactor temperature	= 550°C
pressure	= 16 psia
flow rate	= 10 to 12 l/min.

The start up of Run #6 was somewhat erratic due to a premature turning off of the synthesizer furnace. The run lasted for 10 hours and served to demonstrate a full day of simulated solar furnace operation.

At a meeting held on May 17 with Sandia personnel it was agreed that a set of five eight-hour runs would be made on consecutive days with a minimum of system perturbations during start-up and shut-down in an effort to simulate continuous unattended solar operation for several days and to determine what type of problems might develop.

Run #7 through Run #11, conducted during a one week period, represent the attempted unattended solar simulation. During these experiments it was planned that gas loss and make-up would be kept to a minimum. Shut-down at the end of a day was achieved by turning off the dissociator furnace power and the compressed air supply required to operate the circulation pump. Start-up on the next day was accomplished by the reverse of this procedure without any transfer of additional gases. At night the SO₃ line was kept warm and both furnaces were kept at about 100°C to prevent SO₃ condensation. The intended operating conditions for these experiments were:

dissociator reactor temperature	= 925°C
synthesizer reactor temperature	= 550°C
pressure	= 16 to 18 psia
flow rate	= 10 to 12 l/min.

Run #7 was initiated at 6:00 A.M. on July 9, 1984 and proceeded smoothly for eight hours. There was no loss of pressure during this run and no gas was added to the system. The dissociator furnace was turned down to 100°C and the compressor was turned off at 2:15 P.M. Run #8 was started early the following day without any problems and without any addition of gas. After achieving operating temperatures in the reactors, the line pressure was the same as for Run #7 the day before. During the course of Run #8 there were some indications of loss of power converted as determined by the temperature of the synthesizer.

It was necessary to add a small amount of heat (~20 volts on the variac) to the synthesizer furnace in order to maintain the reactor temperature. For the previous run the furnace had been off during stable operation. Run #8 lasted for the planned eight hours. At the end of the run pressure readings were taken with the compressor operating and with it turned off for comparison. It was noted that the pressure increased by about 1.5 psi when the compressor was turned off due to the pressure indicator location being upstream of the compressor (see Figure 4). To a first approximation, it would be expected that the total pressure drop throughout the loop should not be more than twice this amount or about 3 psi.

Run #9 was started early the following day. At the start of the run a definite loss of pressure was noticed, and small deposits of a dark sludge at low points in the lines were evident. It was surmised that these deposits might be due to the presence of condensed SO_3 or sulfuric acid and dispersed platinum catalyst. The system was purged with the pre-mixed SO_2 and O_2 and pressurized to 16 psi. Two hours into Run #9 the pressure had dropped to 14 psi and a check for leaks was performed. A small leak was located in one of the compressor seals and was repaired by tightening of the cylinder clamping bolts. After again pressurizing the system to 16 psi, no more gas was added during Run #9 which was carried out for the full eight hours.

Run #10 was carried out for eight hours the following day without any problems.

For Run #11 it was necessary to add sufficient make-up feedstock to raise the pressure by 3 psi in order to compensate for an overnight loss due to a leak in one of the fittings. The experiment then continued smoothly for the full eight hours. A check performed on the gas analyzer at the end of Run #11 showed that both the span and the zero readings on the instrument were still correct after a week of operation.

Run #12, performed on August 22, included additional lengths of teflon lines to simulate a longer transport system. A coiled, twelve-foot length of the 12-mm teflon tubing was added in each of the two legs of the closed loop in an effort to determine any possible effect the increased length might have on system operation. The coil added in the SO₃ transport line was heated by an electrical heating tape. During the ten-hour length of this run, several different dissociator temperatures were used. The system pressure was recorded at 19 psi and the flow rate was 11 l/min. during most of the run. At the end of the run the 12-foot coils of teflon tubing were visually inspected and found to be clean and dry. The only difference in system operation noted during Run #12 was an appreciable decrease in the vibrational amplitude of the rotameter ball. This is attributed to the buffering effect of the increased system volume.

V. Results and Discussion:

Graphs showing time base plots of temperature and gas composition data for all of the experiments (except Run #4) are contained in the Appendix of this report. Specific results for each of these tests are discussed briefly, after which general results and comments are presented.

Run #1 - Figures 11, 12, and 13 from the first system check-out experiment demonstrate the successful operation of the furnaces and instrumentation. The effectiveness of the heat exchangers is evidenced in Figure 11 by the difference in temperature between the thermocouples found in the dissociator furnace area (TC-5,6,7) and the thermocouple attached to the first loop of the dissociator heat exchanger (TC-8) as indicated for the dissociator in Figure 5. Without adequate heat exchange thermocouple TC-8 would be expected to increase more in temperature than the increase indicated in Figure 11. A similar observation can be made from Figure 12 for the synthesizer heat exchanger effectiveness. Figure 12 also shows the inactivity of the initial catalyst as the reactor temperatures, indicated by thermocouples TC1 to TC3, cannot be sustained at the operating level ($>500^{\circ}\text{C}$) whenever the power to the furnace is cut down. Once ignition or initiation of the synthesizer reaction has been accomplished the temperature should be sustained by the synthesis process, allowing for small losses to the environment. The catalyst inactivity is further evidenced by the dissociation fraction levels

being almost identical in both the synthesizer and dissociator lines. If both of the processes were working properly a significant difference in the dissociation fractions would be observed between both ends of the loop. The value of the dissociation fraction corresponds to an operating temperature of about 625°C for the synthesizer reactor. However, without dissociation taking place in the dissociator, the synthesis process is not able to sustain reactor temperature due to lack of dissociated gases for synthesis. The fact that synthesis was apparently taking place suggests that the Engelhard catalyst in the dissociator was deactivated during the short time of Run #1 at the high dissociation temperatures. This hypothesis was further supported by consultation with the catalyst manufacturer who indicated that this specific catalyst was not intended for operation at these temperatures as the 12% silica content of the catalyst support would begin to sinter. Our results confirmed this. The catalyst beads originally intended for use in these experiments were of 100% alpha alumina and would reportedly perform satisfactorily at the temperatures intended for these experiments.

From the results of Run #2 (Figures 14-16), the effectiveness of the Matthey-Bishop catalyst is apparent. The relatively high synthesizer temperatures resulted in correspondingly high synthesizer dissociation fractions. The drop in dissociation fraction in the dissociator outlet at $t = 9$ minutes cannot be adequately explained. It

may have been due to sampling technique error. The concentration measurement times used in this run were of the order of the Dupont instrument time constant. The sampling technique was changed in subsequent experiments to permit longer concentration measurement times.

Run #3 - This was the first run with no serious system problems. Both reactors were turned so as to have a vertical orientation for the reactor axes and the flow was from bottom to top in the catalyst beds. The time intervals for performing the SO_2 concentration measurements were increased from one minute to five minutes with alternation between the synthesis and dissociation lines. It should be pointed out that thermocouple TC-1 on the synthesizer was located near the bottom of the converter tube such that it was next to the interface between some inert catalyst beads (used to help retain the active catalyst beads) and the active catalyst beads (see Figure 5). Consequently, this region of the converter tube ran slightly cooler. Thermocouples TC-2 and TC-3 were opposite active catalyst beads. Calculations performed indicate that during the latter half of Run #3 about 330 watts of power was being converted.

Run #5 - As this was intended to be a "long-term" experiment, no meaningful SO_2 concentration measurements were obtained due to the mode of operation as explained in section IV. This run proceeded smoothly with remarkable thermal stability for the entire five-hour duration. The

synthesizer furnace power was turned off and the furnace half-shells were opened slightly to permit adequate cooling of the converter. It was estimated that 390 watts of power were being converted, transported, and delivered during most of this run. Heat exchanger stability for both units is also apparent for this run from the temperatures of TC-8 and TC-4 in Figures 20 and 21 respectively.

Run #6 - This run was the first experiment with the system in its final configuration (Figure 4). The ragged start-up of the synthesizer can be attributed to operational error due perhaps to the smoothness in operation of the previous run. It may also be indicative of what can be expected in terms of the control of a thermochemical transport system when changes are made to an existing configuration. This run was only the second time that the system feedstock was made up using the gas proportioner. From the sharp rises in the temperatures of TC-2 and TC-3 at 35 minutes and again at 135 minutes into the run (see Figure 23), it was assumed that synthesizer ignition had occurred and the furnace power was turned off. These actions turned out to be premature and the power was subsequently turned back on. Synthesizer ignition and stabilization eventually took place approximately 200 minutes into the run and the system operated smoothly thereafter. The corresponding stabilization in the dissociation fraction measurements can be seen in Figure 24. During the last two-thirds of this run, approximately 360

watts of power were being converted with stable operation in both furnaces. From observation of Figure 23, it can be seen that during stable operation of the synthesizer the temperature of TC-2 is about 50°C hotter than that of TC-3. The location of TC-2 is opposite the center of the catalyst bed and TC-3 is close to the downstream end of the catalyst bed (see Figure 5). This would indicate that most of the chemical reactivity is taking place in the main portion of the converter, consistent with the conservative design of the reactors.

Run #7 - Runs #7 through #11 comprised the forty-hour, one-week endurance test. The first of these experiments ran smoothly for the eight-hour period with a single exception. Approximately one hour into the run the temperature registered by TC-2 on the synthesizer reactor suddenly, and for no apparent reason, began to drop while the temperature signal from TC-3 increased as shown in Figure 26. It was found that by applying a small pulse of voltage to the synthesizer furnace (approximately 20 to 30 volts on the variac) this temperature inversion turned around and the previous temperature patterns for TC-2 and TC-3 resumed. Evidently the region of maximum chemical reactivity in the catalyst bed of the synthesizer reactor shifted from the mid portion near TC-2 to the downstream end closer to TC-3. The reason for this type of instability is not clear, but a slight increase in the furnace temperature quickly reversed the situation. Perhaps a slight transient

increase in the flow rate associated with valve manipulation during sampling may have required an additional residence time in the reactor such that, because of the flowing stream, synthesis would not ensue until a later time (i.e., a position further along the catalyst bed). An alternate explanation might be a possible decrease in catalytic activity in the center portion of the catalyst bed taking place due to the unexplained drop in temperature. Restoring the temperature in that portion of the catalyst bed by supplying electrical power to the synthesis furnace restored the catalyst activity. This phenomenon was encountered about five times during subsequent runs. The average conversion power for Run #7 was calculated to be 400 watts.

Run #8 - This test also proceeded without any problems. The power converted was slightly lower than on Run #7, 370 watts compared to 400 watts. Since the reactors were operated at the same temperatures for both of these runs, it is possible that a diminishing in the amount of feedstock may have taken place due to imperceptible leaks in the system during the two days of operation without addition of make-up gas. The pressure in the system had decreased slightly from what it had been at the start of the previous day. The possibility of degradation in feedstock is an alternate explanation as prior to Run #9 some sludge was noticed in the lines. This sludge was not analyzed, but it is conceivable that it could be a

product of a side reaction involving only a sulfur-bearing component which would alter the stoichiometric ratio of SO_2 and O_2 and only minimally affect the pressure. Condensation of SO_3 would not alter the stoichiometric ratio and should be more noticeable as a loss in pressure. Unfortunately the pressure monitor for this system was situated at the opposite end of the system from where SO_3 condensation would be most likely to occur.

Run #9 - New gas was introduced into the system at the beginning of this run because of the visible presence in the low points of the system, especially at stopcock valves, of what appeared to be SO_3 condensation or sulfuric acid with dispersed metal-like material in it, perhaps platinum. The purging was thought to be necessary to prevent any possible undesirable reaction as this material could get swept into a high temperature area. Both reactors operated well and no temperature inversions occurred in the synthesizer as evidenced from Figure 32. The peculiar changes in the SO_2 concentrations as seen in Figure 33 cannot be readily explained. It is possible that the Dupont instrument sample cell or its lines may have contained small quantities of condensed liquids and that these materials may have caused the short term drifts in the concentration measurements in both lines. It can be seen from observation of Figures 31, 32, and 33 that a slight modulation in the temperatures of both reactors coincides with the valving back and forth between the two

legs of the loop for gas analysis. This effect is more obvious for the dissociator (Figure 31) and is barely noticeable for the synthesizer (Figure 32). The possibility also exists for the presence of some slight obstruction in the teflon valve in the direct dissociator line such that shunting the flow through the analyzer instrument would actually reduce the back pressure and more dissociation would take place in the dissociator to compensate for this slight reduction in pressure in keeping with Le Chatelier's principle. The effect that an obstruction would have on the flow rate and the resulting changes on other parameters would be difficult to quantitate for the present system. The power converted during this run was calculated to be 385 watts using a conservative value for $(F_2 - F_1)$ of 0.70 (Equation 2).

Run #10 - The first five hours of this fourth consecutive day of operation proceeded without incident with a calculated power conversion of 375 watts. Two of the synthesizer temperature inversions discussed above were experienced during the last three hours of this run as seen in Figure 35. Both of these were successfully inverted by applying a five to ten minute pulse of voltage power as described earlier for Run #7. The effect of these temperature inversions is apparent in the SO_2 concentration readings (Figure 36). It is surmised that when the chemical reactivity is taking place close to the end of the catalyst bed some of the material gets by unreacted due to

the lack of sufficient residence time in the synthesis reactor. This could account for the higher levels of SO₂ detected.

Run #11 - An obvious feature of the graphs for Run #11 (Figures 37-39) is the loss of the data logger for 30 minutes. This minor annoyance had no effect on the experiment. During the last half of the test, three synthesizer reactor temperature inversions were experienced. The first two were detected and reversed early while the third developed more fully. This allowed more SO₂ to pass through unreacted as seen in Figure 39 towards the end of the graph. The mean power conversion during this run was calculated to be 410 watts.

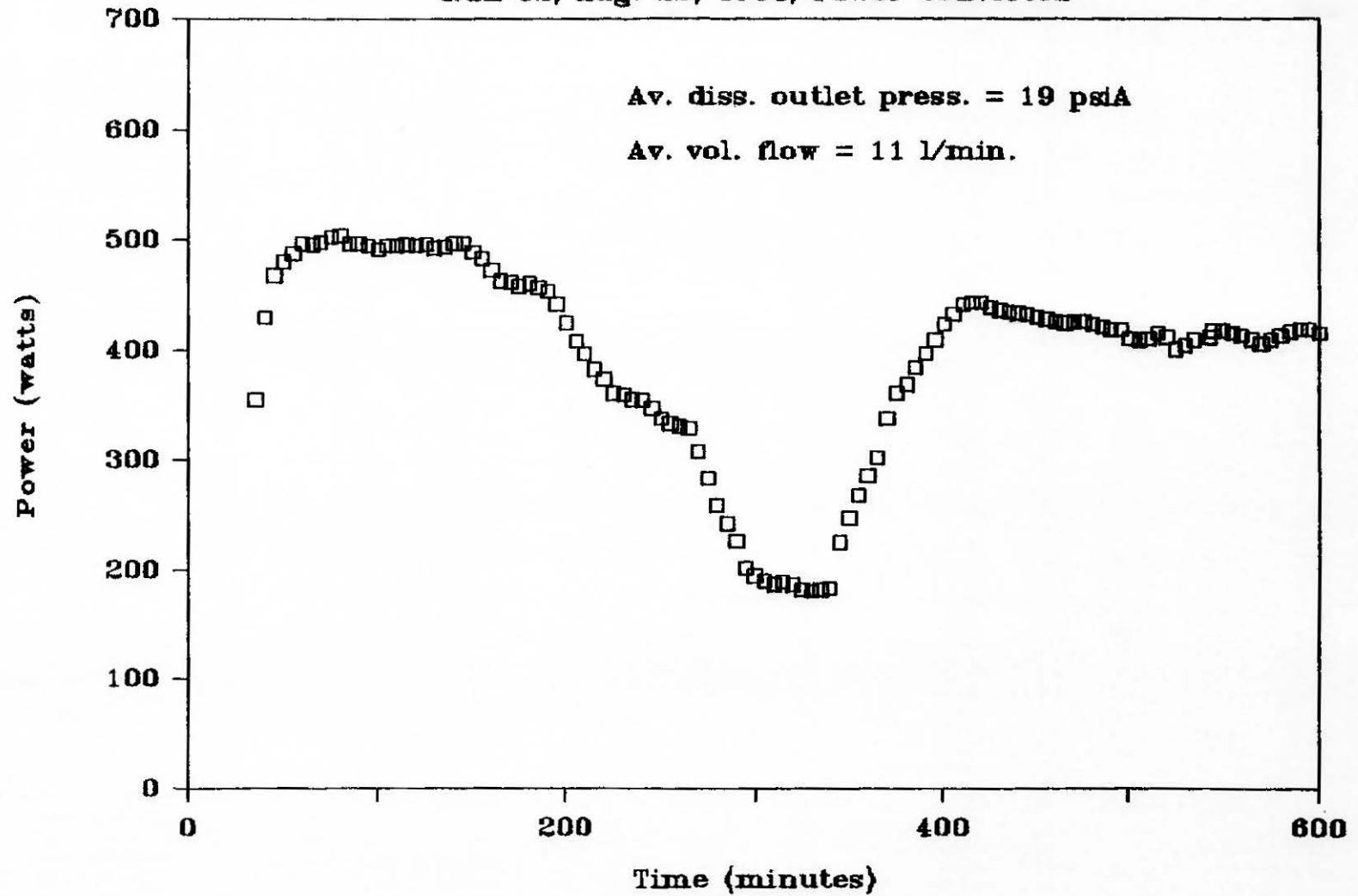
Run #12 - Prior to this experiment the system lines were disconnected in order to insert two twelve-foot coils of teflon tube to test operation with longer transport lines. In addition to the longer transport lines, the temperature of the dissociator was varied during the course of this run. Figure 40 shows the dissociator temperature slowly increasing to 1000°C, holding for an hour, followed by one-hour periods at 900°C and 800°C, then increasing to 950°C for the remainder of the run. The dissociator heat exchanger reached equilibrium rather quickly and closely followed the temperature profile of the dissociator reactor. The dissociation fraction curve

for the dissociator outlet (Figure 42) follows an unanticipated profile when compared to the dissociator temperature profile from Figure 40. The increase in the SO_2 concentration with temperature up to 950°C was as expected, but the apparent decrease on ramping up to 1000°C was not expected. Although increments in the dissociation fraction are more difficult to achieve at these high temperatures, as evidenced from an inspection of the SO_3 dissociation curve in Figure 1, the apparent decrease goes against what one would predict for this reaction. Another interesting feature of the dissociation fraction curve for this run is the decrease in the SO_2 levels when compared to the levels at equivalent temperatures under 950°C achieved in previous runs. This may be indicative of dissociator catalyst deactivation and can be attributed to the brief exposure to temperatures above 1000°C .

Using equation 2 to determine the power converted from the dissociation fraction data of Figure 42, the power curve shown in Figure 7 was obtained as a function of time for the ten-hour experiment. The most important feature of this graph is the constant power conversion of 500 watts from 50 to 150 minutes into the run followed by a slight drop during the next 50-minute period. During the first 200 minutes of operation the mean temperature of the dissociator was increased to and held at approximately 1000°C (see Figure 40). The power converted then decreased further as the temperature of the dissociator was lowered

SANDIA SOLAR THERMAL

Run 12, Aug. 22, 1984, Power Converted



42

Figure 7: Run #12 Power Converted

to 900°C and held for an hour and then to 800°C and held for an hour. When the temperature was raised back up to 950°C at about 400 minutes into the run, the power converted never regained its initial value of 500 watts. This behavior also suggests that the catalyst may have been damaged due to the exposure to temperatures above 1000°C. This catalyst material had not been previously exposed to temperatures that high in any of the previous runs. Figure 41 shows the temperature profile for the synthesizer reactor. The synthesizer furnace was off during the entire run except for the short period from 300 to 350 minutes (while the dissociator furnace was at 800°C) and again for a few minutes during the synthesizer temperature inversion at about 520 minutes. It is interesting to note that TC-2, adjacent to the center of the synthesizer catalyst bed, roughly follows the temperature profile of the dissociator. This behavior would be expected if indeed this portion of the synthesizer were responding to the supply of dissociated gases from the dissociator, i.e., the reduced amount of reactants was producing less synthesis and consequently less heat was being produced resulting in a lowered temperature. One might then expect TC-3 to follow a similar profile below that of TC-2. The fact that TC-3 does not trail below TC-2 could be explained in part by a shift of the reaction front from the area close to TC-2 to that closer to TC-3 (downstream). The coincidental application of external

heat to the synthesizer at this time should also have a bearing on the response of TC-2 and TC-3. Perhaps TC-2 would have dropped lower in temperature but did not due to the external heat application, while TC-3 may be displaying the combined effects of synthesis heat output and external heat application. The SO_2 concentration data for the synthesizer outlet (Figure 42) are more in keeping with exit temperatures above 500°C . An interesting and important implication of this behavior for solar applications is the possibility of loose coupling or decoupling of the dissociator and synthesizer reactors in an operating system, especially one with a larger buffering capacity. This small-scale experiment, because of the inability to adjust heat removal from the synthesizer to compensate for a reduced heat generation, is apparently not able to sustain the synthesis reaction when the feed-stock reactant composition drops below the equilibrium concentration level for the given temperature. A larger-scale system with a higher buffering capacity would be capable of maintaining the reaction conditions and the required equilibrium concentrations for longer periods of time. In essence it would have a much longer time constant for the system.

After Run #12 was completed and the system had cooled, the reactors were removed from their furnaces for inspection. It was noted that the dissociator catalyst beads had changed from their original black color to a light

shade of gray and some of the beads were nearly white. No discoloration was observed for the synthesizer catalyst beads upon inspection. Although the discoloration could be strictly cosmetic in nature, when taken in conjunction with the reduced dissociation activity it lends support to the conjecture that the dissociator catalyst may have been damaged due to the exposure above 1000°C. Since there was no detectable change in the overall reactivity of the dissociator until Run #12, it is strongly believed that the Matthey-Bishop catalyst used in these experiments is good up to but not above 1000°C, at least for time periods up to the length of these experiments.

The following general comments and observations were offered by the experimenters after completion of the closed-loop, bench-scale, laboratory tests.

1. Most system problems could be related to leaks into or out of the system. The accumulation of small quantities of acid in the system, the loss of feed-stock, and the changes in stoichiometry could be eliminated if the system were completely free of leaks that allow the escape of reactant gases as well as allow moisture to creep in.
2. If the SO₃ line is heat traced, the condensation of small quantities of SO₃ appears to be only a minor, manageable problem.
3. The synthesizer temperature inversions observed in some of the later experiments are not completely

understood. The data gathered in these experiments suggests the existence of an ignition front within the synthesizer catalyst column. The front was observed to move downstream within the bed during some of the later runs. When this happened, the highest temperature occurred at the end of the reactor, suggesting a decrease in the effective volume of the catalyst and total reactivity decreased. Since providing external heat by turning on the synthesizer furnace for a brief period of time would apparently restore the reaction front to the central position, it is suggested that a small preheater at the inlet of the synthesizer might help to eliminate this problem.

4. There was definite evidence of dissociator catalyst deterioration during the last experiment. The Matthey-Bishop MB-3 material appears to work quite well at the temperatures below 1000°C used in these experiments. It seems fairly certain, however, that the platinum catalyst on the alumina beads is affected on exposure to about 1000°C. Analytical work on this catalyst is currently underway at Sandia.
5. It can be said based on the results of the last six experimental tests that, in general, system operation is easy to initiate and maintain. With the exception of occasional synthesizer temperature inversions, long-term system operation in the order of several

days is stable and reliable. The problem encountered with losses of feedstock attributed to leakage would require more careful attention on a larger system in order to minimize it. It is advantageous that the cost of the feedstock does not represent a major capital expense. Changes in stoichiometry can be corrected during operation, if necessary, by the use of a gas proportioner (this worked well during the tests).

VI. Conclusions and Recommendations:

Most of the original contract objectives listed in section II were accomplished during the course of this project. The most notable exception was the failure to study the effect of short-term interruptions to system operation. The purpose of that objective was to determine the effect of a cloud passing over a solar plant under full operation. It was agreed early in the project to make an exception to this particular contract objective for the following reasons: The heat capacity of the dissociator furnace used in these experiments was quite large; i.e., hours rather than minutes were required to cool the reactor from 900°C to a temperature well below that of the synthesizer. The only way to achieve rapid cooling of the dissociator would have been to remove the quartz reactor/heat exchanger assembly from the furnace. Both system and safety considerations suggested that this

mode of operation would not be prudent. Provisions should be made in any follow-on experiments to address this phenomenon.

Another exception was the failed attempt to study the effect of pressure changes on the system. Due to the nature of the joints between the teflon and the quartz tube of the reactor/heat exchanger assemblies, attempts to implement significant pressure increases led to disconnections at these joints with resultant losses of feedstock. A third exception was the failure to provide experimental data that would give a direct measure of the system energy delivery efficiency. It was found that the system did not lend itself to calorimetric measurements at the synthesizer. These three items are areas that definitely need to be addressed in any follow-up work with the SO_3 system for thermochemical transport.

Based on the results of the present work, it is concluded that the dissociation of SO_3 and the synthesis of its products in a closed loop system present a viable means for converting, transporting, and recovering solar energy as high temperature heat. Although the size of the system reported here is small, it contained all of the elements of a much larger energy plant. It is held by the present workers that the laboratory closed loop could be scaled upward by a factor of ten or twenty in terms of power converted and that the operation and analysis of such a larger system would provide important data to the

design and operation of a solar-powered pilot plant.
Problem areas suggested by the present work are: (1)
dissociator catalyst maximum operating temperatures and
(2) synthesizer catalyst bed instabilities.

ACKNOWLEDGEMENTS

The authors wish to acknowledge the analytic and consultative services provided by Dr. T. A. Chubb of Research Systems, Inc., Oxon Hill, MD. In addition to providing consulting services to the project, RSI prepared a "Thermochemical Energy Transport Handbook, SO₃" (26) which proved to be a valuable analytical tool.

VII. References:

1. J. F. Muir, "Economic Analysis of Thermochemical vs. Sensible Energy Transport for Distributed Receiver Solar Thermal Systems," Sandia National Laboratories Report SAND84-2013 (to be published).
2. K. Kugeler, H. F. Niessen, M. Roth-Kassat, D. Bocker, R. Ruter, and K. A. Theis, . "Transport of Nuclear Heat by Means of Chemical Energy (Nuclear Long Distance Energy)," Nuclear Engineering and Design, 34, 65-72 (1975).
3. "Reversible Chemical Reactions for Electrical Utility Energy Applications," Final Report, Contract TPS-76-658, prepared by Rocket Research Corporation, Redmond, WA, for EPRI, Palo Alto, CA, April 1977.
4. H. B. Vakil and J. W. Flock, "Closed Loop Chemical Systems for Energy Storage and Transmission (Chemical Heat Pipe)" Contract No. EY-76-C-02-2676, (1978).
5. O. M. Williams and P. O. Carden, "Screening Reversible Chemical Reactions for Thermochemical Energy Transfer," Solar Energy, 22, 191, (1979).
6. R. L. Graves, "Screening Study of High Temperature Energy Transport Systems," ORNL/TM-7390, October, 1980.
7. J. V. Fox, "Thermochemical Energy Transport Systems Study," Final Report Number JCS-PR-002 Sandia National Laboratories Contract No. 47-4034, (4 November 1983).
8. J. M. Schredder, "Performance and Cost of Energy Transport and Storage Systems for Dish Applications Using Reversible Chemical Reactions," report No. DOE/JPL-1060-79 (October 15, 1984).
9. R. D. Smith, "Chemical Energy Transport for Distributed Solar Thermal Electric Conversion," RRC 81-R-782, Final Report, Contract No. 18-2563 (SAND81-8190), (February 1982).
10. W. E. Wentworth and E. Chen, "Simple Thermal Decomposition Reactions for Storage of Solar Thermal Energy," Solar Energy, 18, 205, (1976).
11. M. L. Bhakta, "Chemical Storage of Thermal Energy Using the $\text{SO}_3\text{-SO}_2\text{-O}_2$ System," M.S. Thesis, U. C. Berkeley, December 1976.
12. S. H. Kalfayan and H. E. Marsh, "Chemical Energy Storage Systems Screening and Preliminary Selection," JPL Report No. 5105-40 (August 1980).

13. T. A. Chubb, Analysis of Gas Dissociation Solar Thermal Power Systems, Solar Energy, 17, 129 (1979).
14. T. A. Chubb, J. J. Nemecek and D. E. Simmons, Application of Chemical Engineering to Large Scale Solar Energy, Solar Energy, 20, 219 (1978).
15. T. A. Chubb, J. J. Nemecek and D. E. Simmons, Design of a Small Thermochemical Receiver for Solar Thermal Power, Solar Energy, 23, 217 (1979).
16. T. A. Chubb, Characteristics of CO₂-CH₄ Reforming-Methanation Cycle Relevant to the Solchem Thermochemical Power System, Solar Energy, 24, 341 (1980).
17. J. H. McCrary, Gloria E. McCrary, T. A. Chubb, and Yong S. Won, An Experimental Study of SO₃ Dissociation as a Mechanism for Converting and Transporting Solar Energy, Solar Energy, 27, 433 (1981).
18. J. H. McCrary, Gloria E. McCrary, and T. A. Chubb, An Experimental Study of the CO₂-CH₄ Reforming Methanation Cycle as a Mechanism for Converting and Transporting Solar Energy, Solar Energy, 29, 141 (1982).
19. Kirk-Othmer, Encyclopedia of Chemical Technology, 3rd Edition, Vol. 22, pp 191-199 (1980).
20. L. J. Weirick, "Oxidation/Sulfidation of Material Candidates for Distributed Solar Receiver Thermochemical Transport Program in SO₂/O₂," Sandia National Laboratories Report SAND 85-0757 (June 1985).
21. L. J. Weirick, "Oxidation/Sulfidation of Material Candidates for Distributed Thermochemical Transport Program in SO₃," Sandia National Laboratories Report SAND 85-2091.
22. Solar Thermal Hydrogen Production Process, Westinghouse Electric Corporation, Advanced Energy Systems Division, Final Report for USDOE, Contract No. DE-ACD2-78ET20608 (1982).
23. E. W. Schmidt, Development of a Long-Life High-Temperature Catalyst for the SO₂/SO₃ Energy Storage System, Rocket Research Co., Report No. RRC-*0-R-697 (1980).
24. Y. S. Won, G. E. Voecks, and J. H. McCrary, Experimental and Theoretical Study of a Solar Thermochemical Receiver Module, DOE/JPL Document No. 1060-76 (1984).
25. J. H. McCrary and Gloria E. McCrary, Evaluation of SO₃ Metallic Converters, Final Report, JPL Contract No. 955704 (1980).

26. T. A. Chubb, Thermochemical Transport Handbook - SO₃, Research Systems, Inc. report (1984).
27. S. Miyamoto, A. W. Warrick and H. L. Bohn, Land Disposal of Waste Gases, J. Environmental Quality, 3, 49 (1974).

VIII. Appendix:

Note: All volume flow readings in the following figures as throughout the text are given at the ambient experimental conditions without correcting to STP.

SO₂ VAPOR PRESSURE

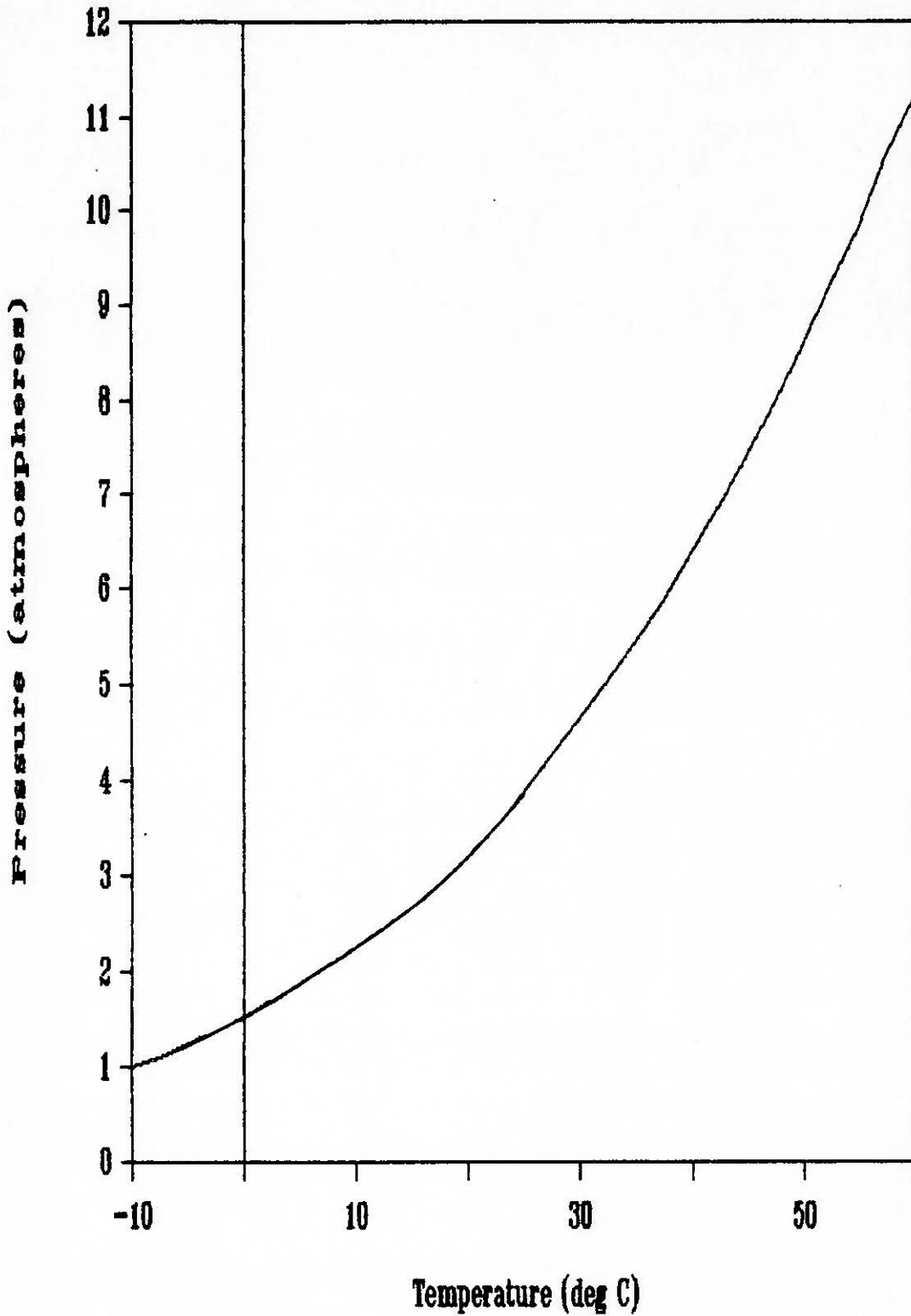


Figure 8: SO₂ Vapor Pressure

SO₃ VAPOR PRESSURE

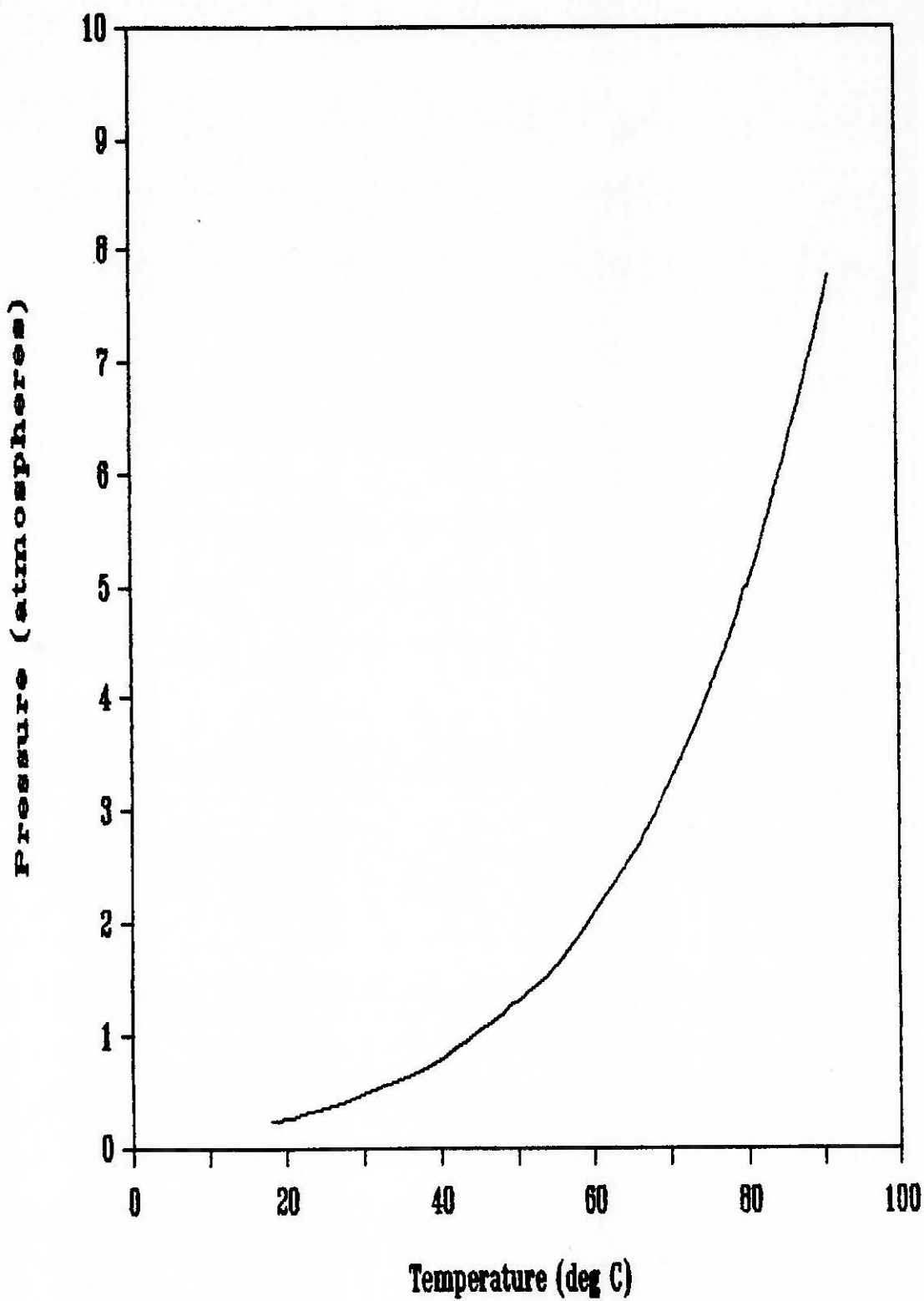
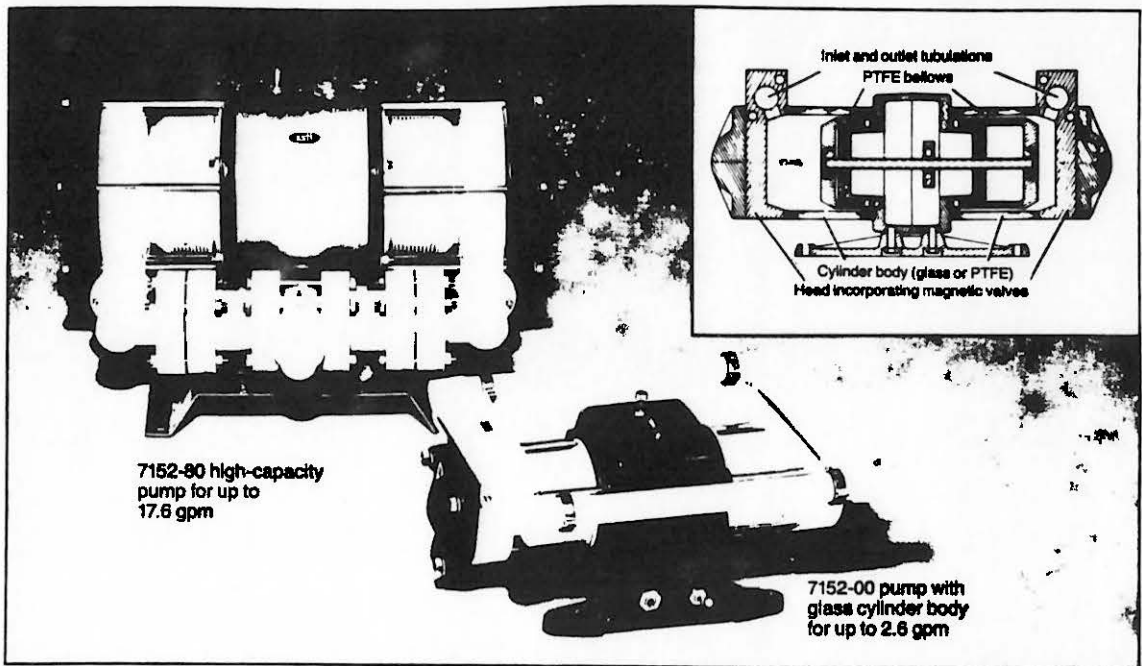


Figure 9: SO₃ Vapor Pressure

Pneumatic Teflon® bellows pump



meet the demanding transfer and metering requirements of chemical manufacturing and processing. Chemical-resistant Teflon TFE wetted parts let you handle corrosives, solvents, and caustics at temperatures between -22° and +266°F (-32° to +130°C). All parts are easy to clean to eliminate cross-contamination.

gases, and mixed phases (liquids with gas bubbles) at differential pressures between 0 and 45 psi. Pumps may run dry without damage.

Pumps operate from a compressed air line or compressor. Use 40 to 60 psi for best results. Order the air filter and regulator at right.

Two pumping chambers, each consisting of Teflon TFE bellows and cylinder (glass or Teflon), are placed opposite each other so that one chamber fills as the other empties. Magnetic inlet and outlet valves seal the chambers between strokes.

Connect air line to the inlet. A pneumatic start/stop switch and speed control regulator are located between pumping chambers for easy access.

0.7 to 2.3 gpm, 1.5 to 5.5 gpm, and 1.5 to 17.6 gpm. Choose models with wetted parts of Teflon and glass, or all Teflon. All models have Teflon O-rings. The clear glass cylinder lets you verify liquid flow at a glance. All-Teflon models handle etching solutions.

- K-7148-63 1/4" (F)NPT for K-7152-00, -10 pumps \$19.60 ea
- K-7148-64 3/8" (F)NPT for K-7152-60, -70 pumps \$19.80 ea
- K-6469-23 1" (F)NPT coupling for K-7152-80, -85 \$30.00 ea

Catalog number	Max gpm	Cylinder material	Dimensions			Shpg wt	Price
			L	W	H		
K-7152-00	2.3	Glass	12.6"	7.1"	5.1"	10 lbs (4.5kg)	\$ 988.00
K-7152-10	2.3	Teflon	12.6"	7.1"	5.1"	10 lbs (4.5kg)	1075.00
K-7152-60	5.5	Glass	15.2"	10.4"	6.7"	20 lbs (9.1kg)	1360.00
K-7152-70	5.5	Teflon	15.2"	10.4"	6.7"	20 lbs (9.1kg)	1566.00
K-7152-80	17.6	Glass	18.9"	18.5"	12.2"	58 lbs (26.4kg)	3180.00
K-7152-85	17.6	Teflon	18.9"	18.5"	12.2"	58 lbs (26.4kg)	3700.00

- K-7042-40 Air filter with 50-micron element.
3/8" ports \$25.70
- K-7042-44 Air regulator with gauge, 0-160
psi, 3/8" ports \$21.15

All flow rates are at maximum air pressure—60 psi

Catalog number	Ports (M)NPT	Input scfm	Differential pressure			
			0 psi	15 psi	30 psi	45 psi
K-7152-00, -10	1/4"	1.25	2.3 gpm	1.8 gpm	1.3 gpm	0.7 gpm
K-7152-60, -70	1/2"	2.36	5.5 gpm	3.9 gpm	2.8 gpm	1.5 gpm
K-7152-80, -85	1"	8.00	17.6 gpm	10.3 gpm	6.3 gpm	1.5 gpm

Teflon—Reg TM E.I. DuPont de Nemours & Co.

17.6 gpm
45 psi
266°F (130°C)
none
Teflon TFE bellows, glass cylinder, Teflon TFE O-rings, Teflon TFE impeller

Figure 10: Teflon Bellows Pump

SANDIA SOLAR THERMAL

Run 1, April 5, 1984, Dissociator Temp.

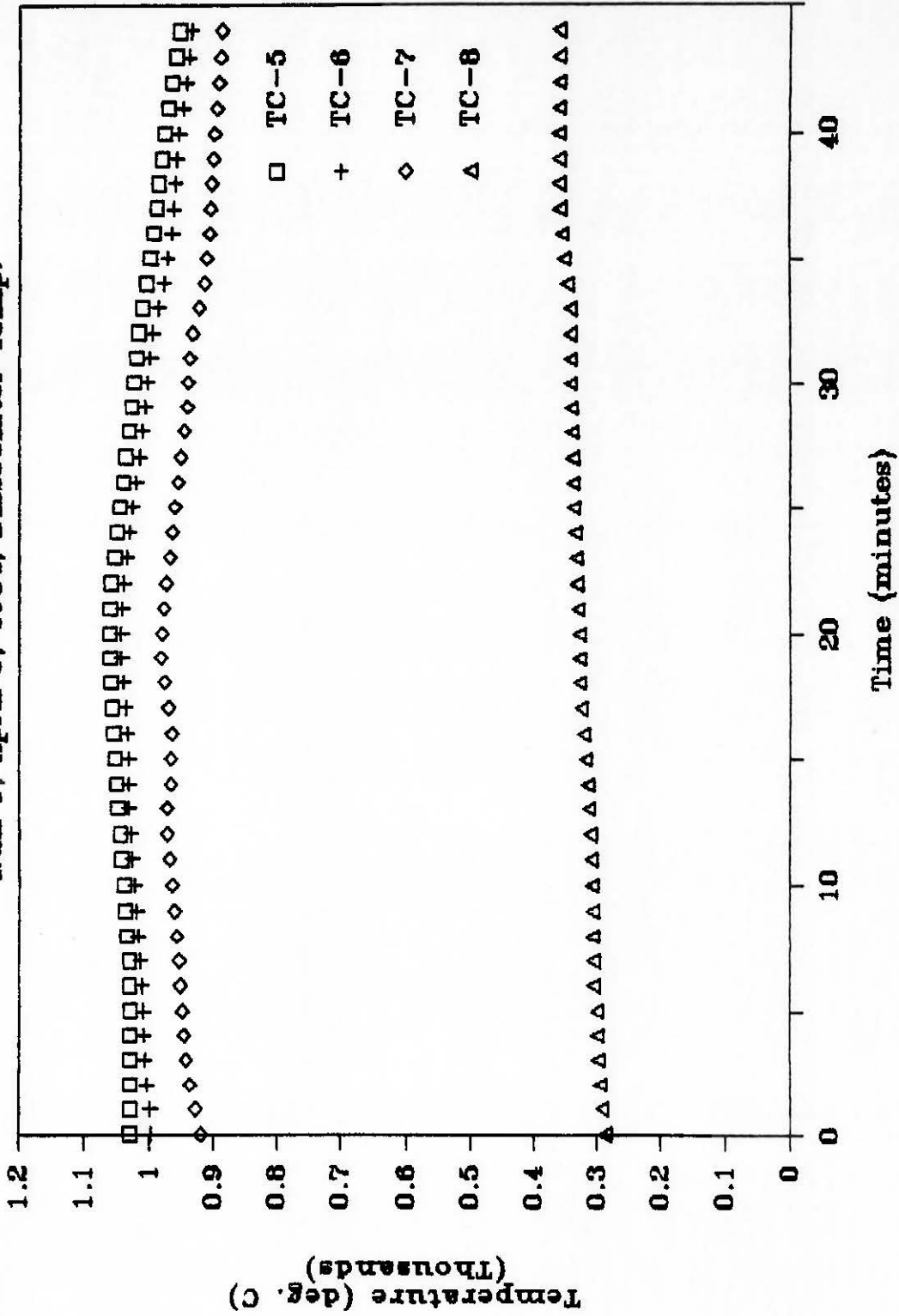


Fig. 11: Run #1 Dissociator Temperatures

SANDIA SOLAR THERMAL

Run 1, April 5, 1984, Synthesizer Temp.

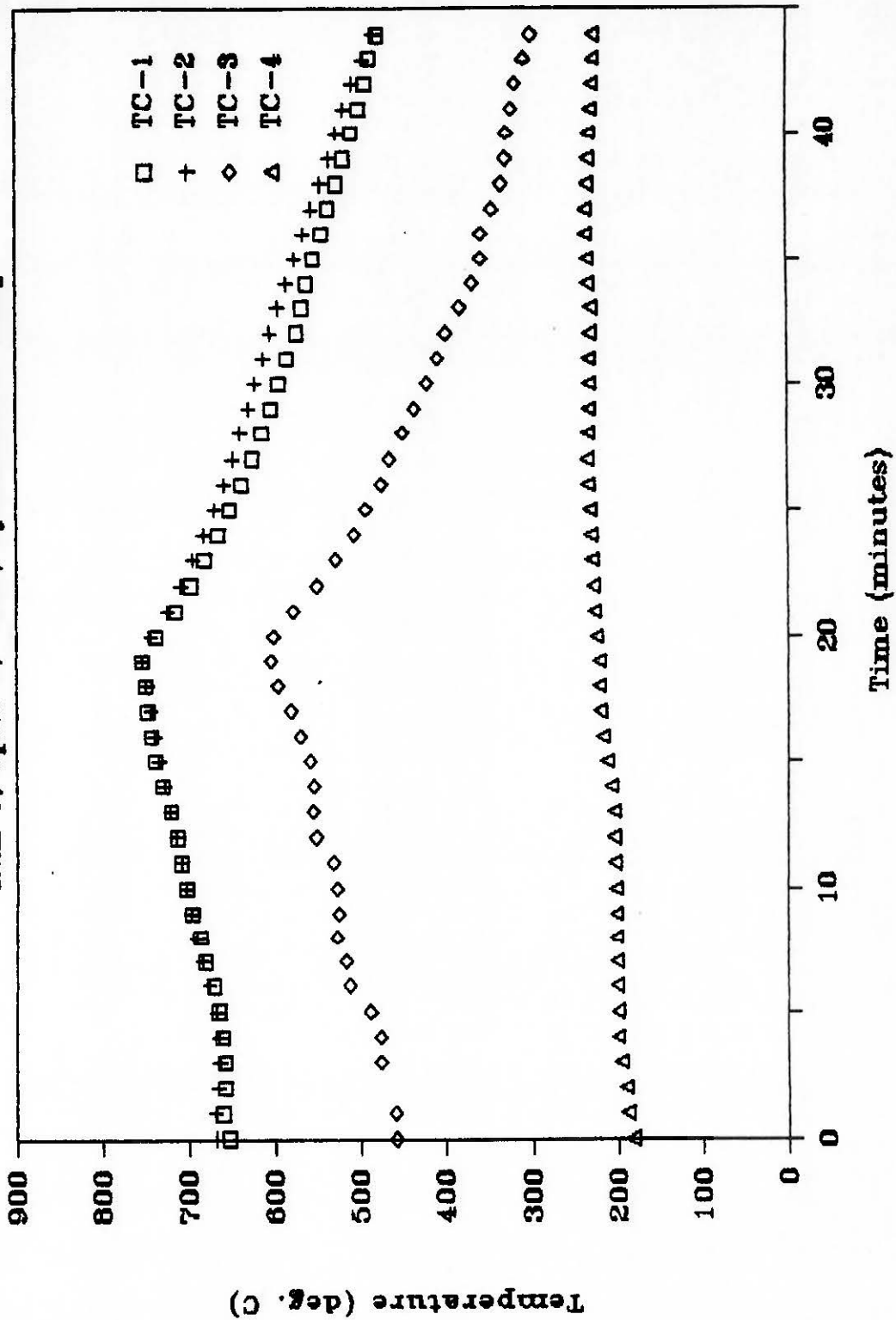


Fig. 12: Run #1 Synthesizer Temperatures

SANDIA SOLAR THERMAL

Run 1, April 5, 1984, SO₂ Concentration

69

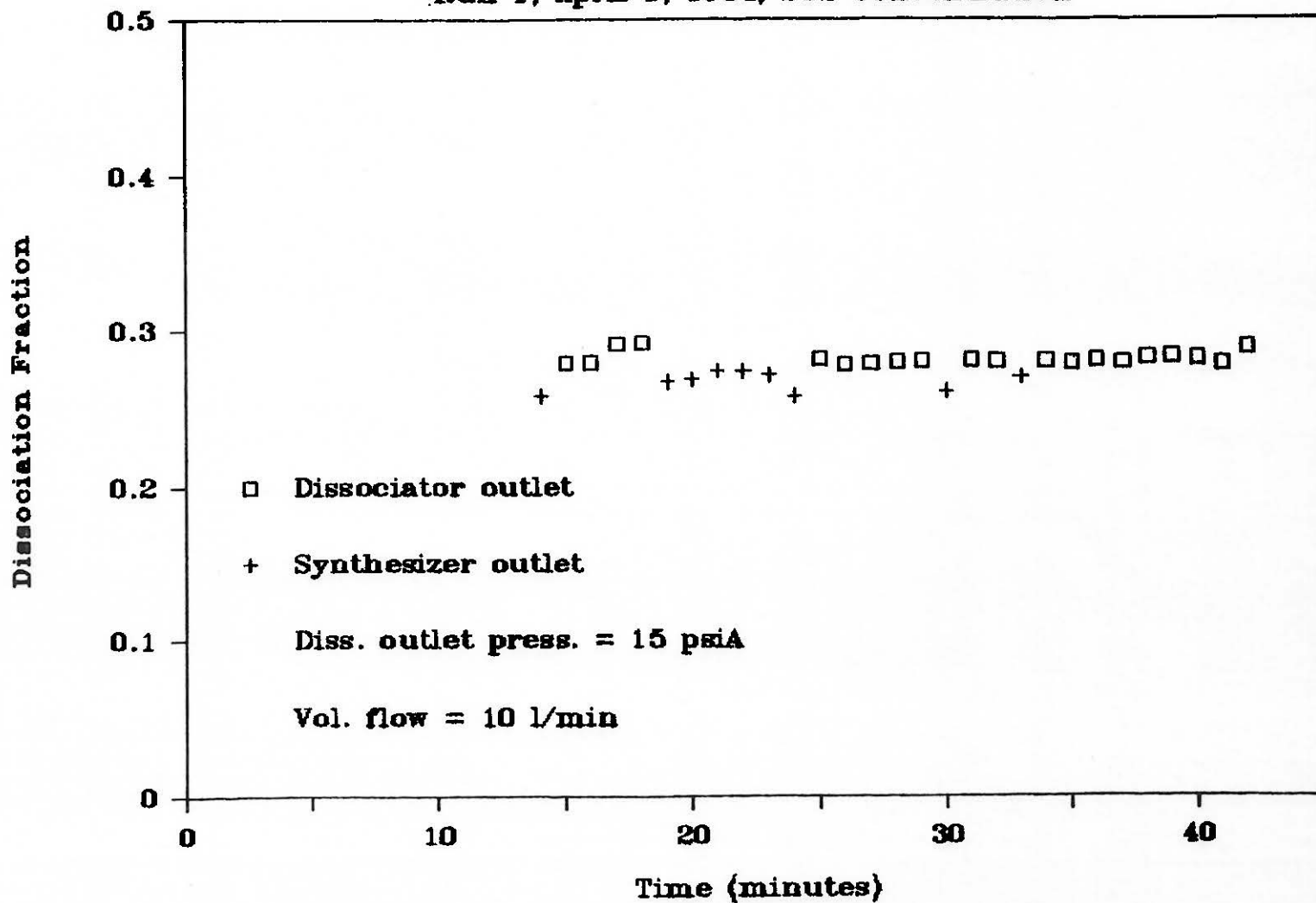


Fig. 13: Run #1 Dissociation Fractions

SANDIA SOLAR THERMAL

Run 2, May 2, 1984, Dissociator Temp.

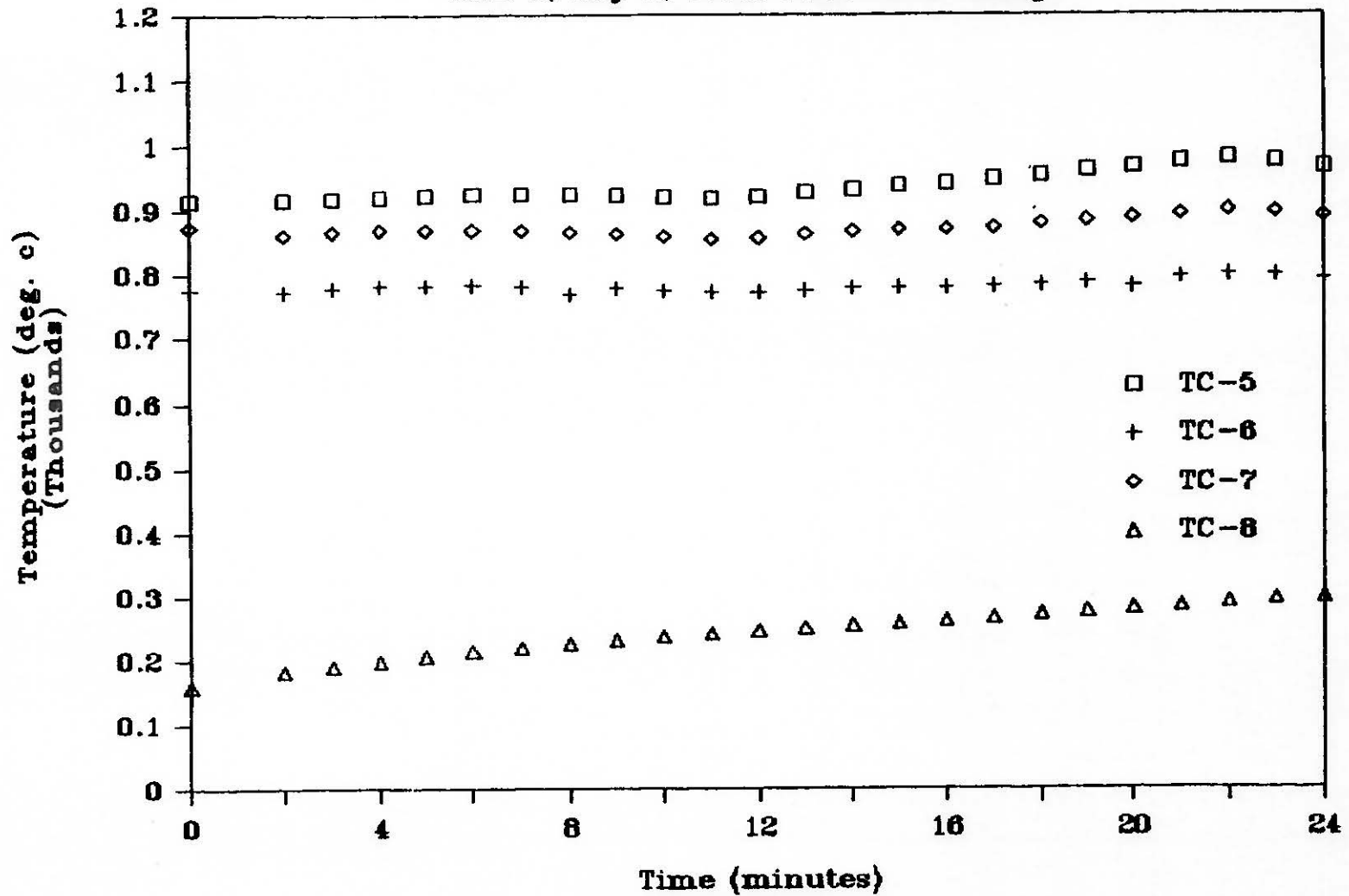


Fig. 14: Run #2 Dissociator Temperatures

SANDIA SOLAR THERMAL

Run 2, May 2, 1984, Synthesizer Temp.

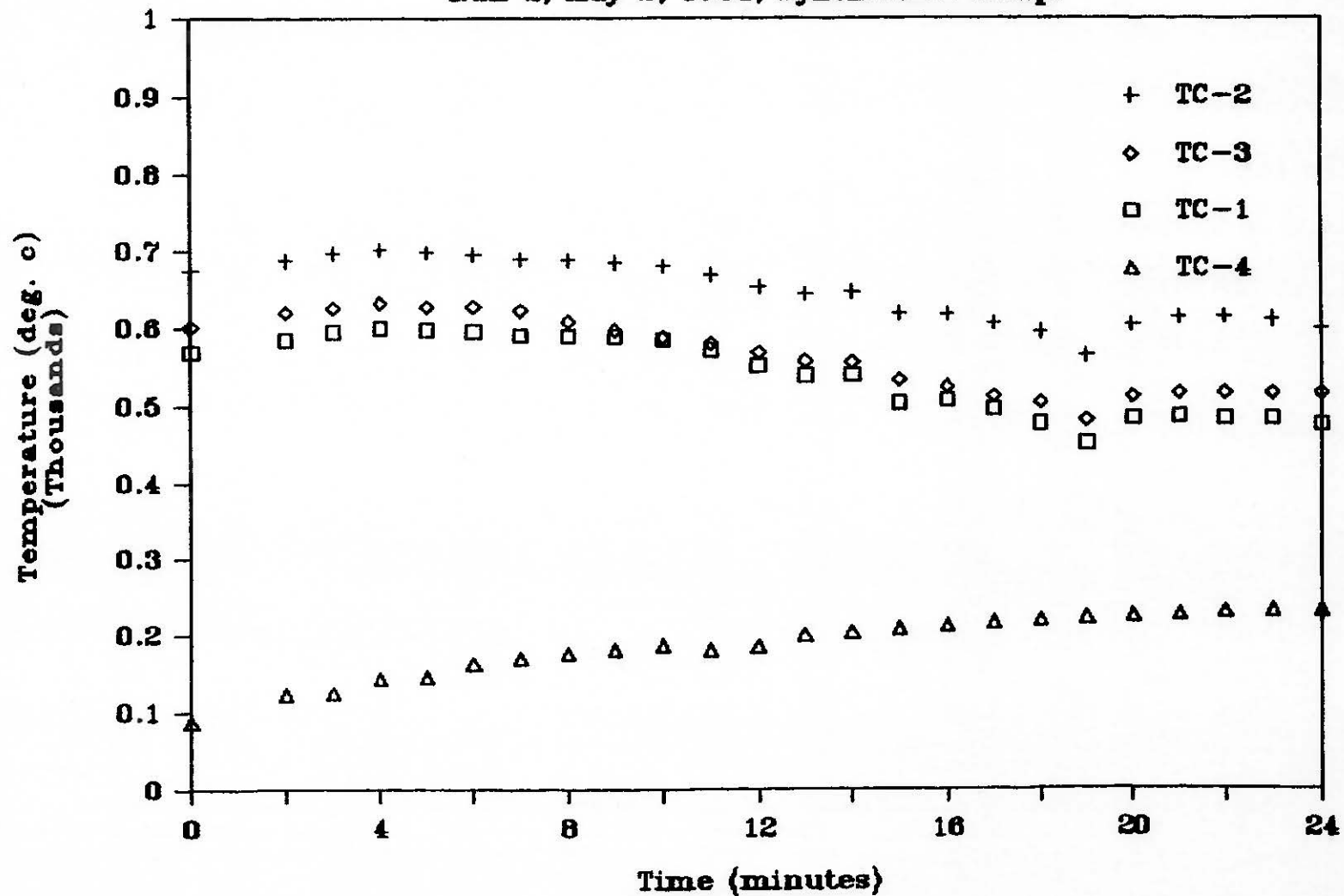


Fig. 15: Run #2 Synthesizer Temperatures

SANDIA SOLAR THERMAL

Run 2, May 2, 1984, SO₂ Concentration

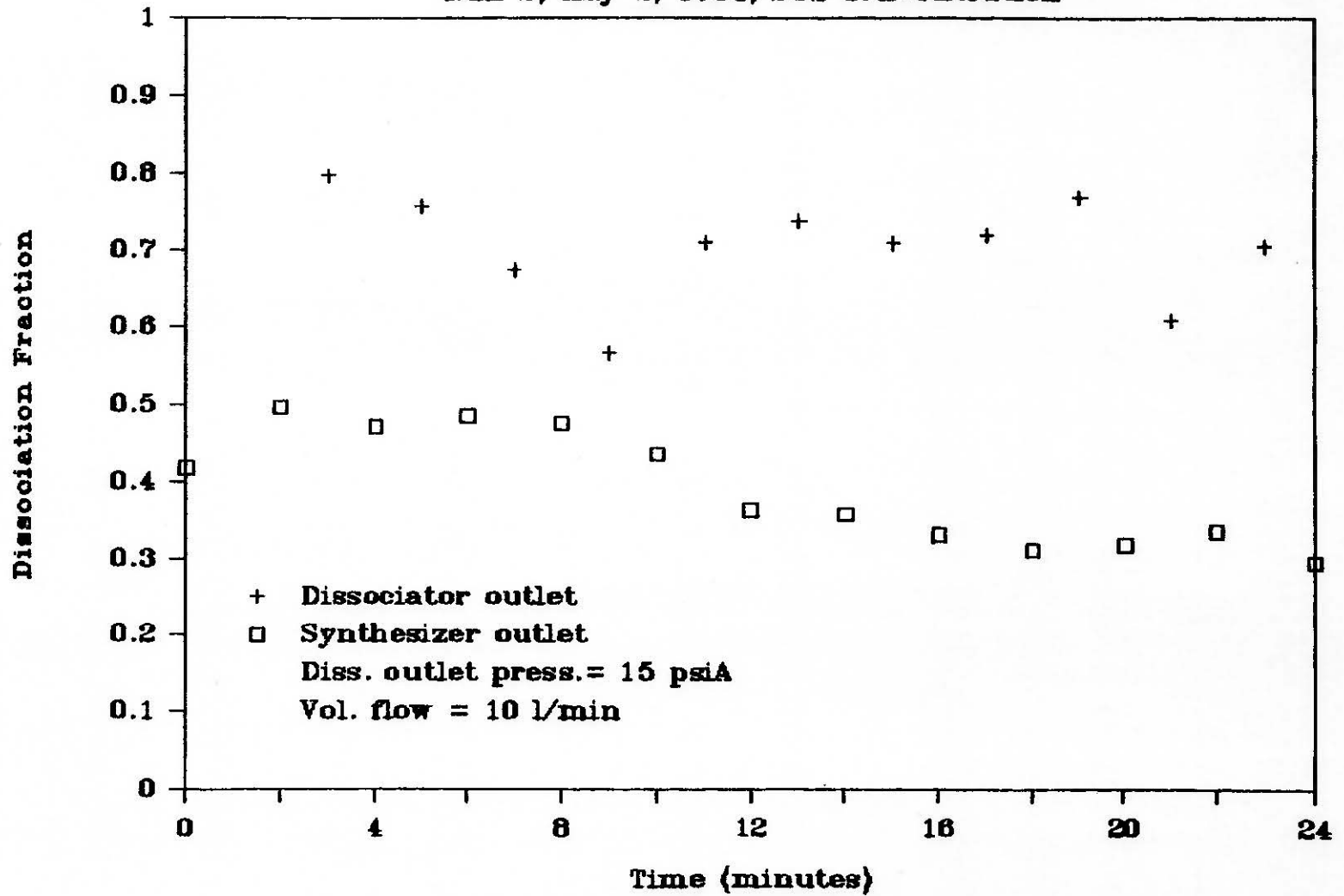


Fig. 16: Run #2 Dissociation Fractions

SANDIA SOLAR THERMAL

Run 3, May 10, 1984, Dissociator Temp.

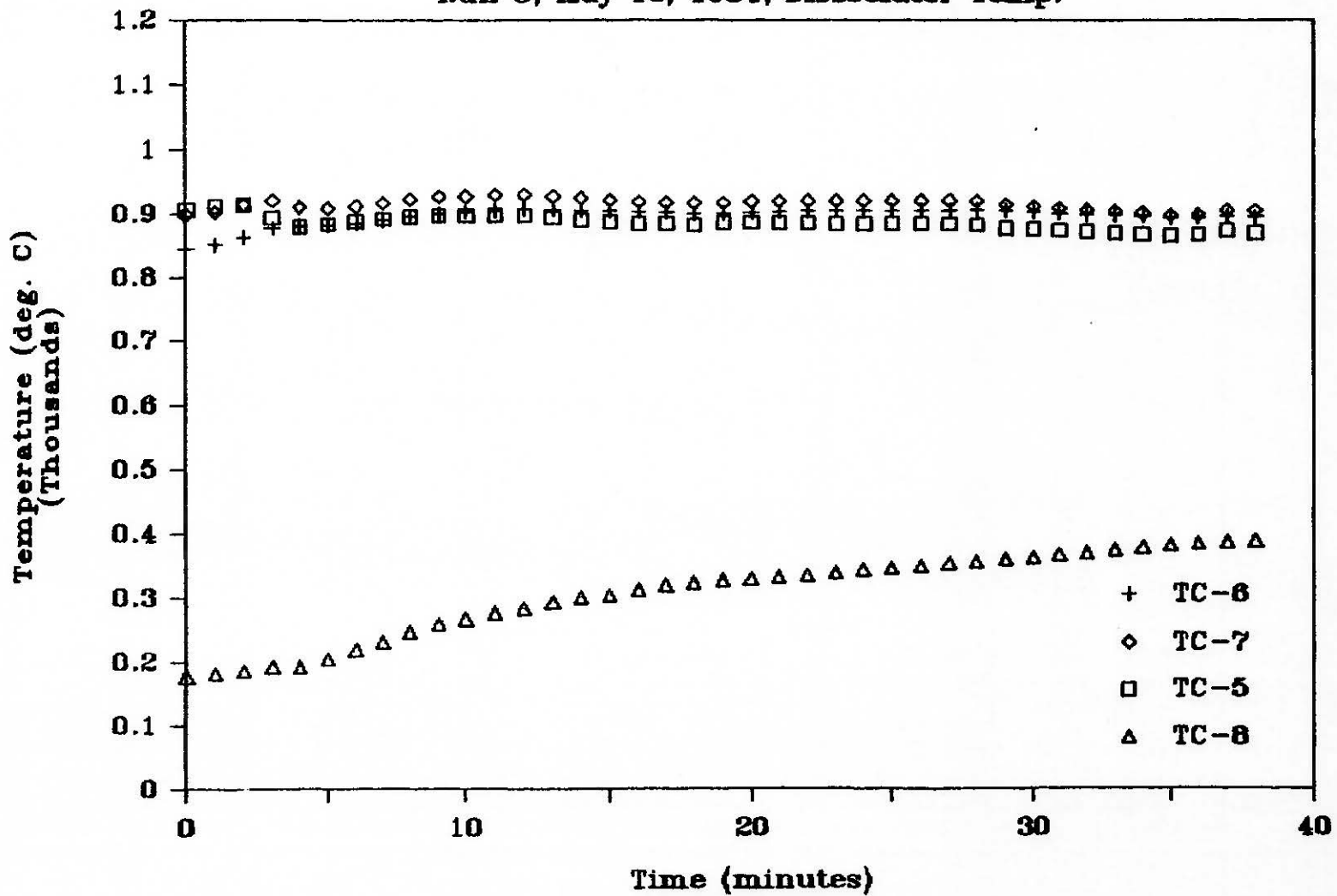


Fig. 17: Run #3 Dissociator Temperatures

SANDIA SOLAR THERMAL

Run 3, May 10, 1984, Synthesizer Temp.

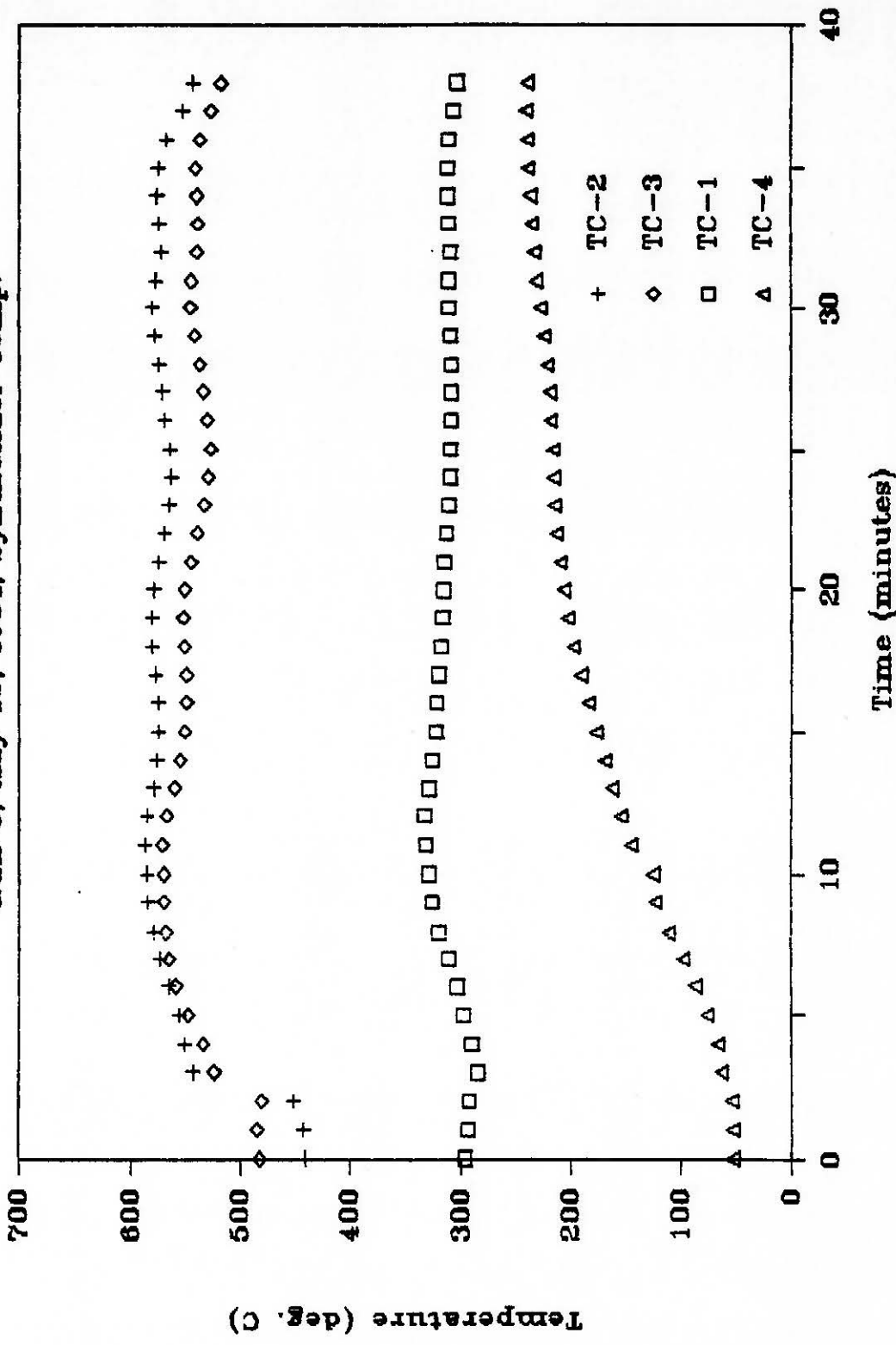


Fig. 18: Run #3 Synthesizer Temperatures

SANDIA SOLAR THERMAL

Run 3, May 10, 1984, SO₂ Concentration

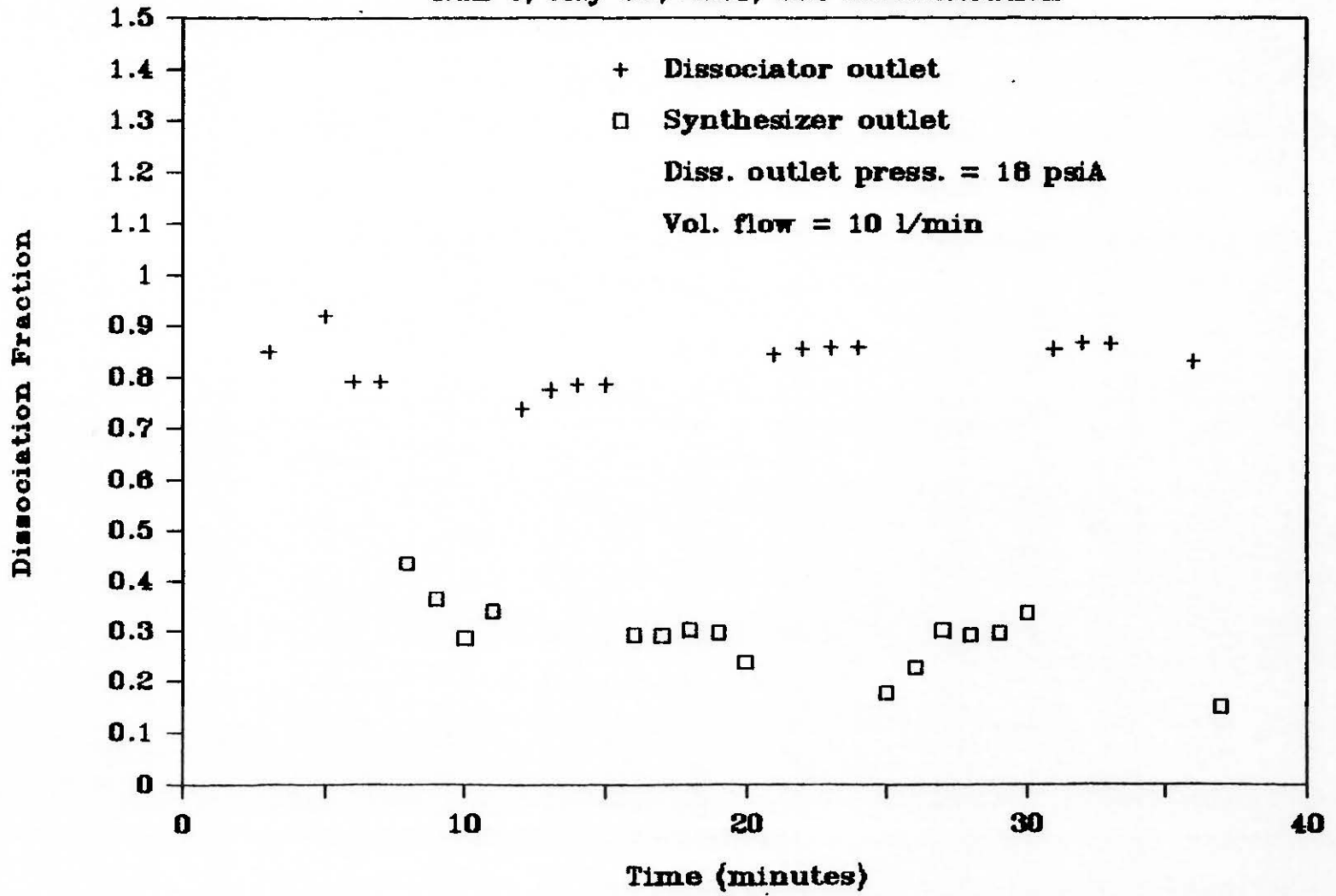


Fig. 19: Run #3 Dissociation Fractions

SANDIA SOLAR THERMAL

Run 5, June 6, 1984, Dissociator Temp.

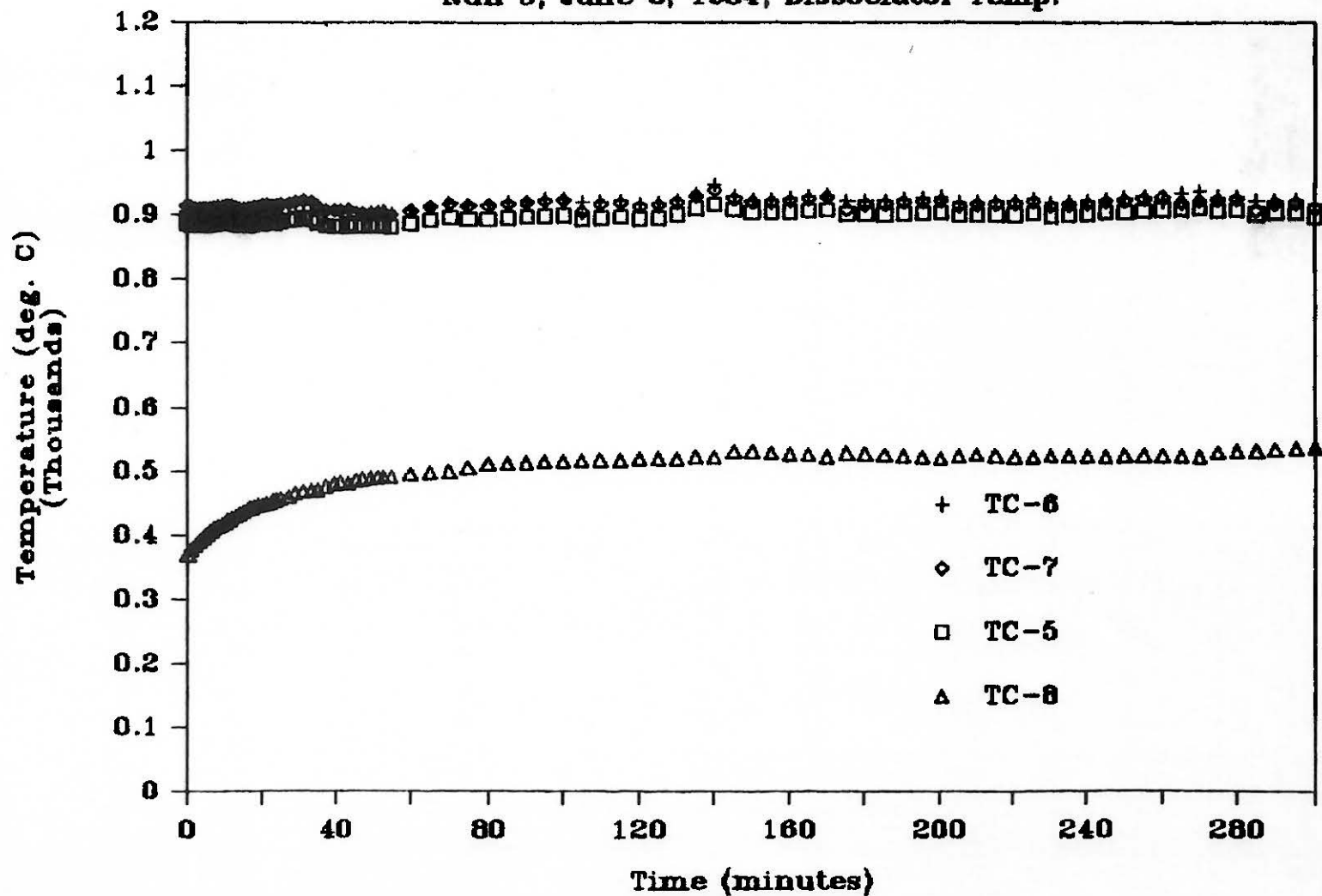
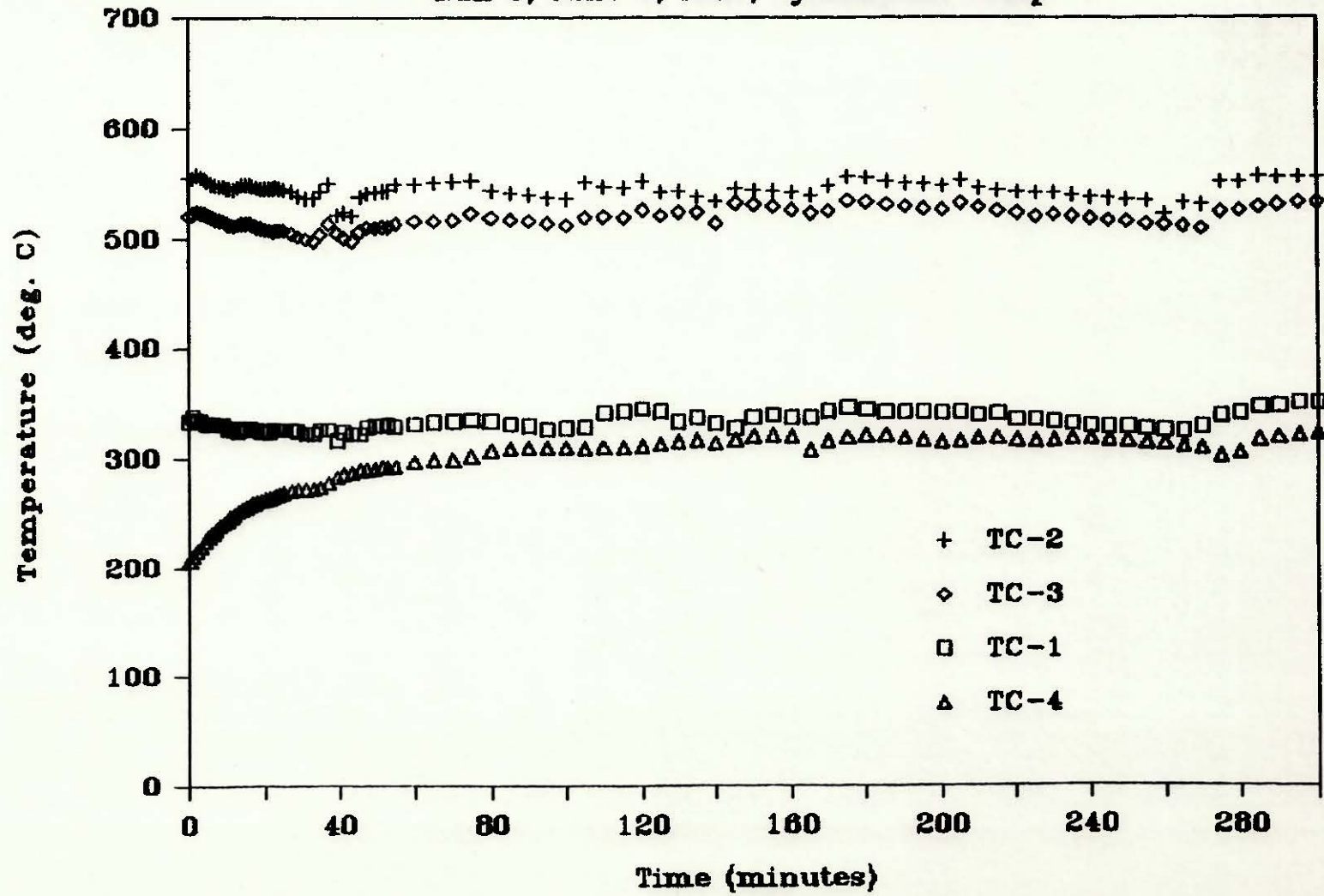


Fig. 20: Run #5 Dissociator Temperatures

SANDIA SOLAR THERMAL

Run 5, June 6, 1984, Synthesizer Temp.



67

Fig. 21: Run #5 Synthesizer Temperatures

Sandia Solar Thermal

Run 6, June 26, 1984, Dissociator Temp.

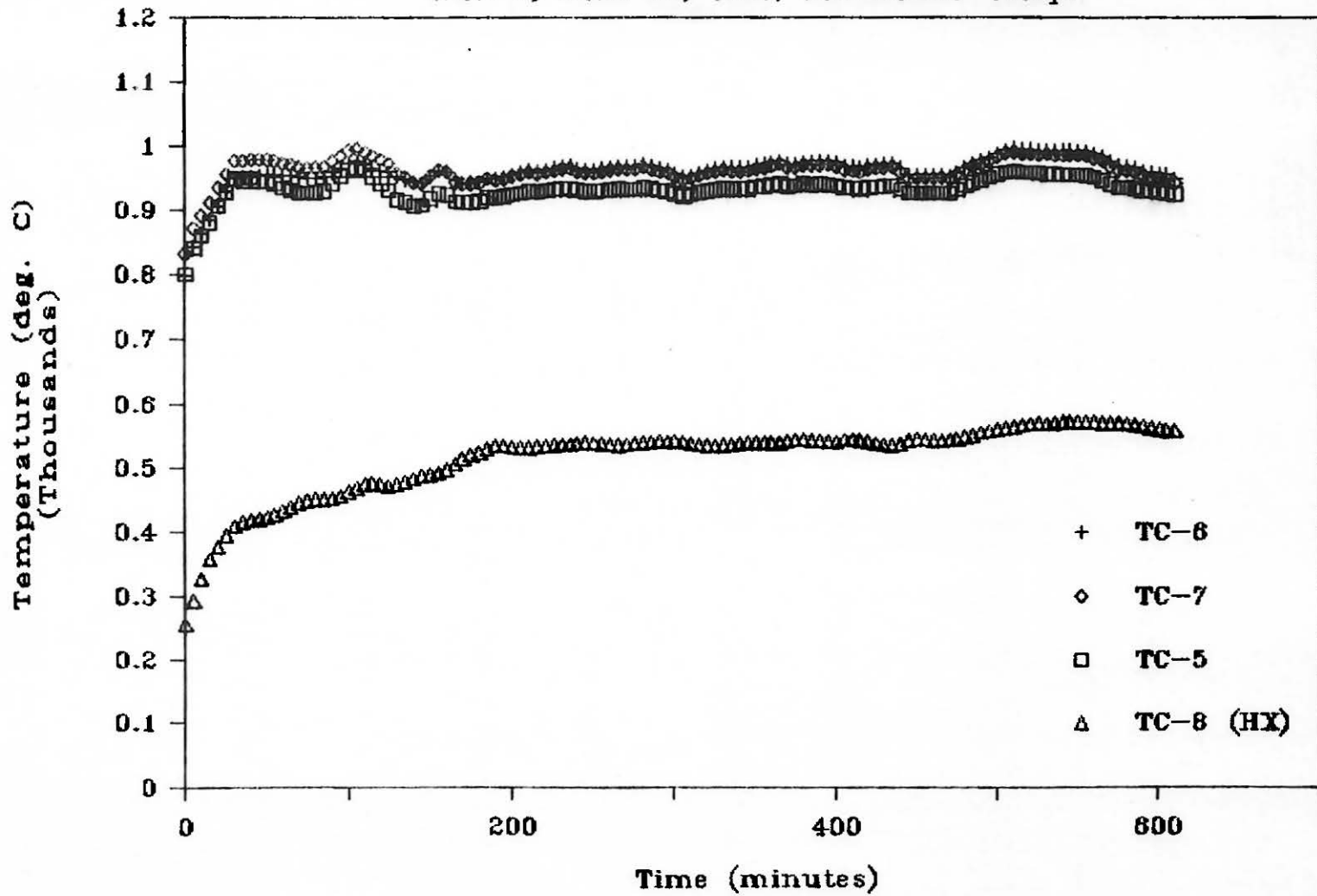


Fig. 22: Run #6 Dissociator Temperatures

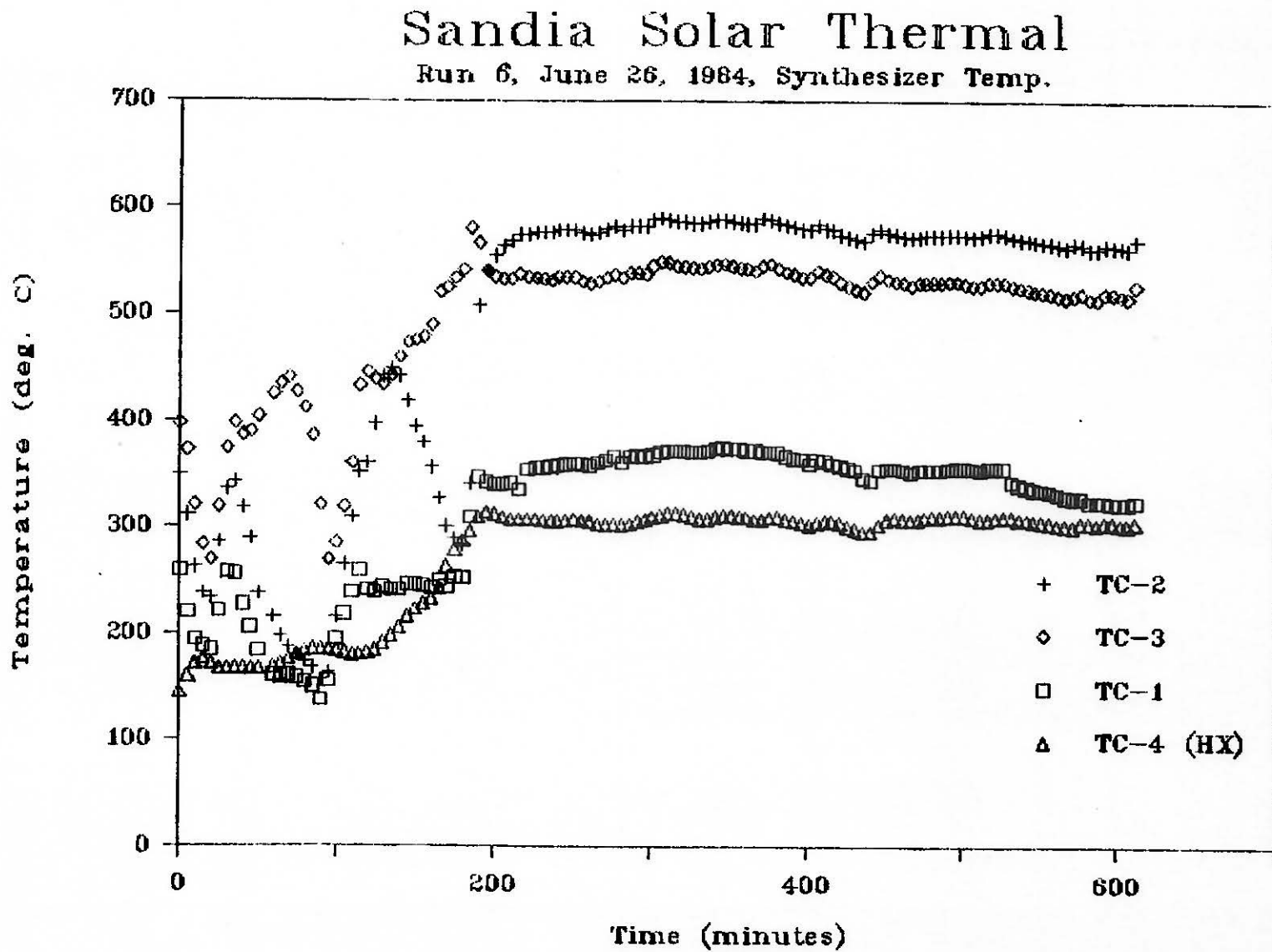


Fig. 23: Run #6 Synthesizer Temperatures

Sandia Solar Thermal

Run 6, June 26, 1984, SO₂ Concentration

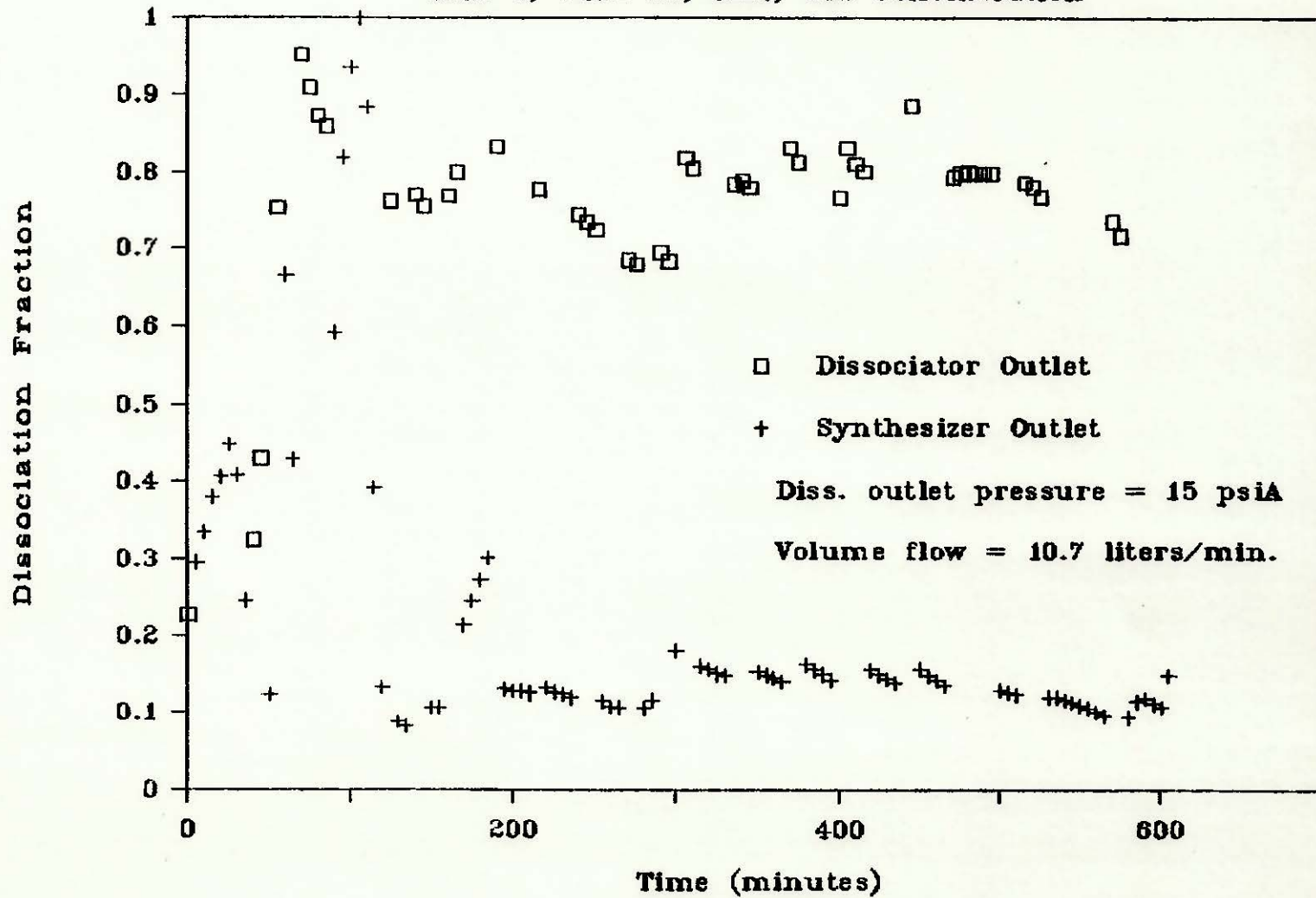


Fig. 24: Run #6 Dissociation Fractions

SANDIA SOLAR THERMAL

Run 7, July 9, 1984, Dissociator Temp.

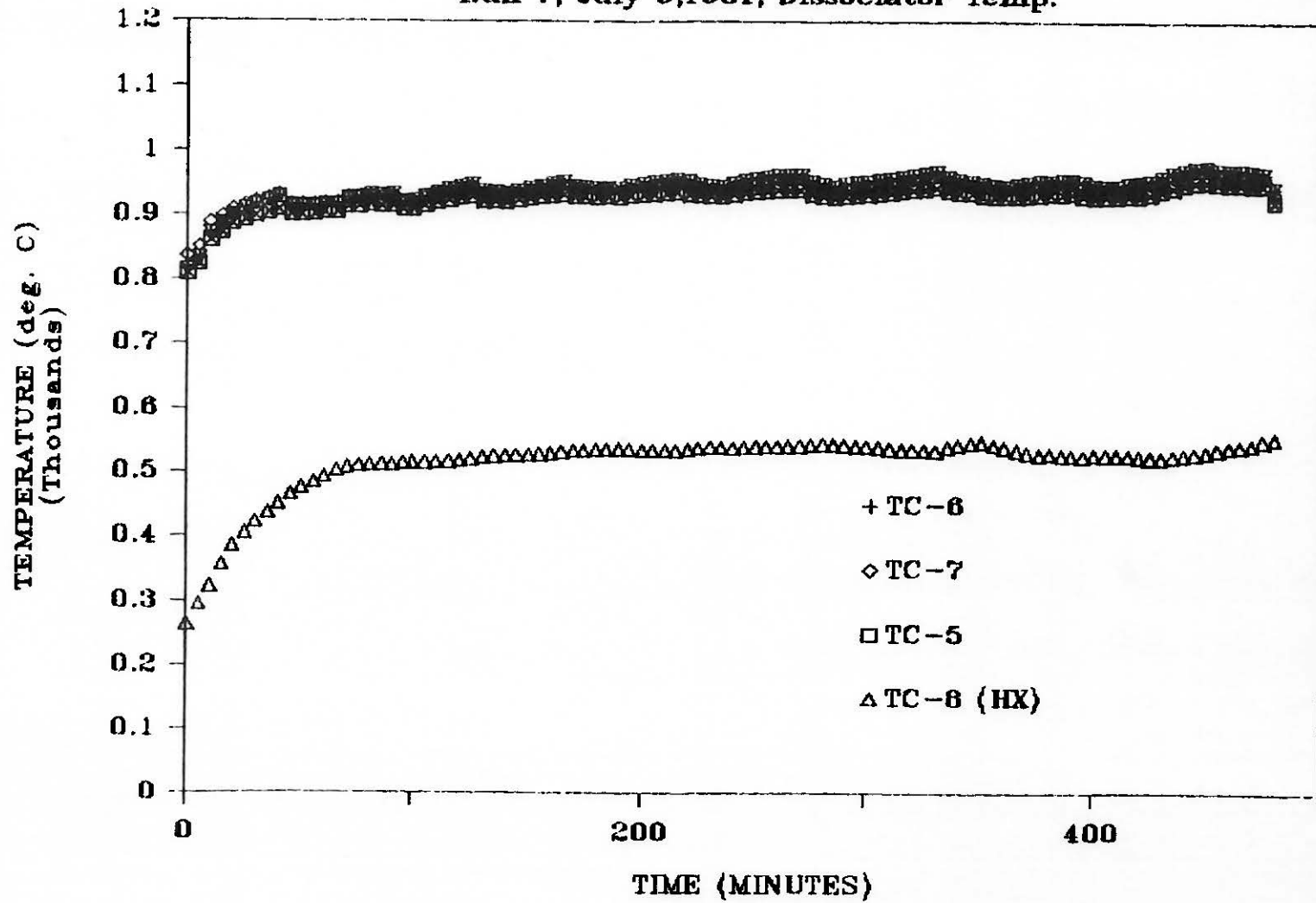


Fig. 25: Run #7 Dissociator Temperatures

SANDIA SOLAR THERMAL

Run 7, July 9, 1984, SO₂ Concentration

73

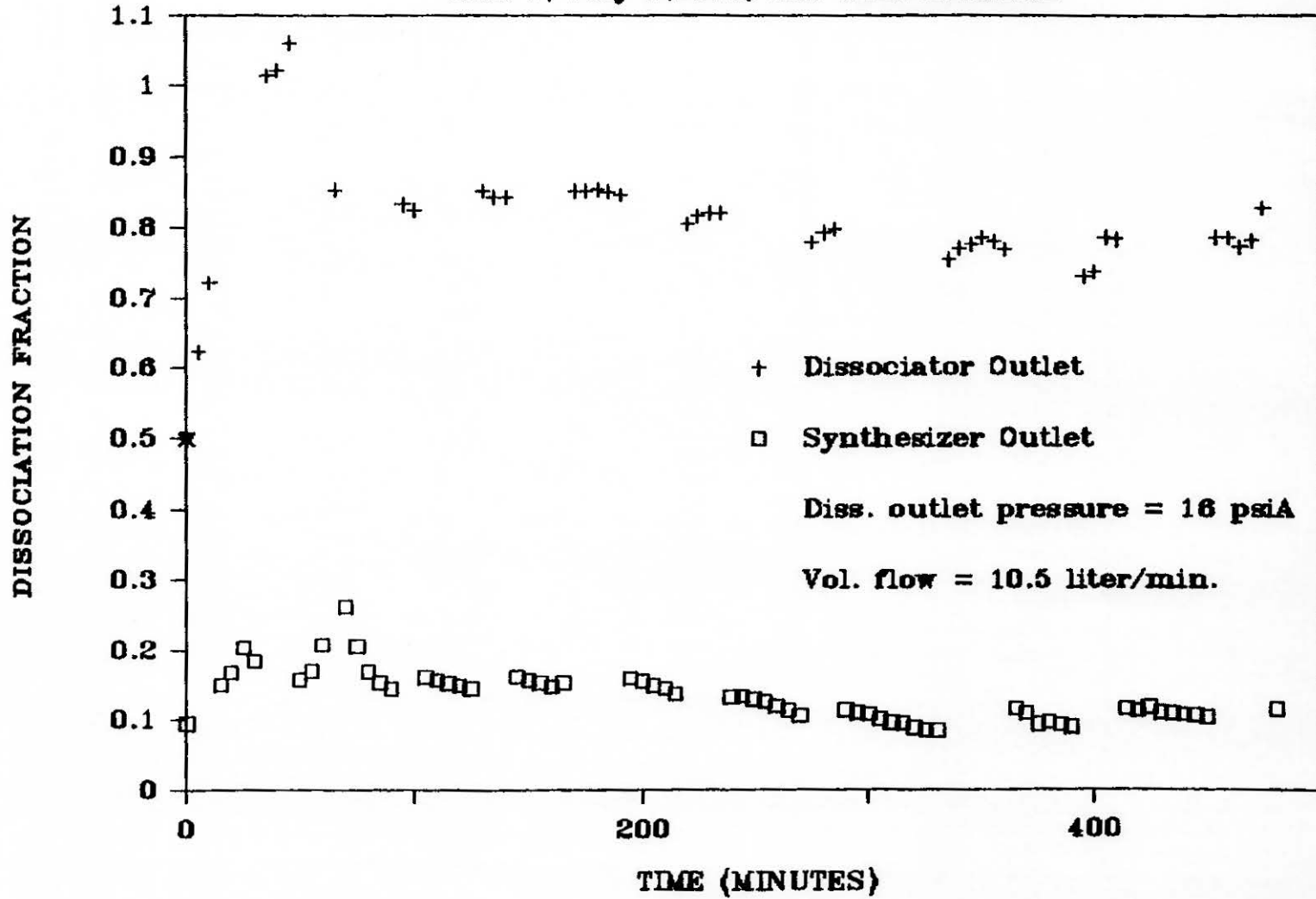
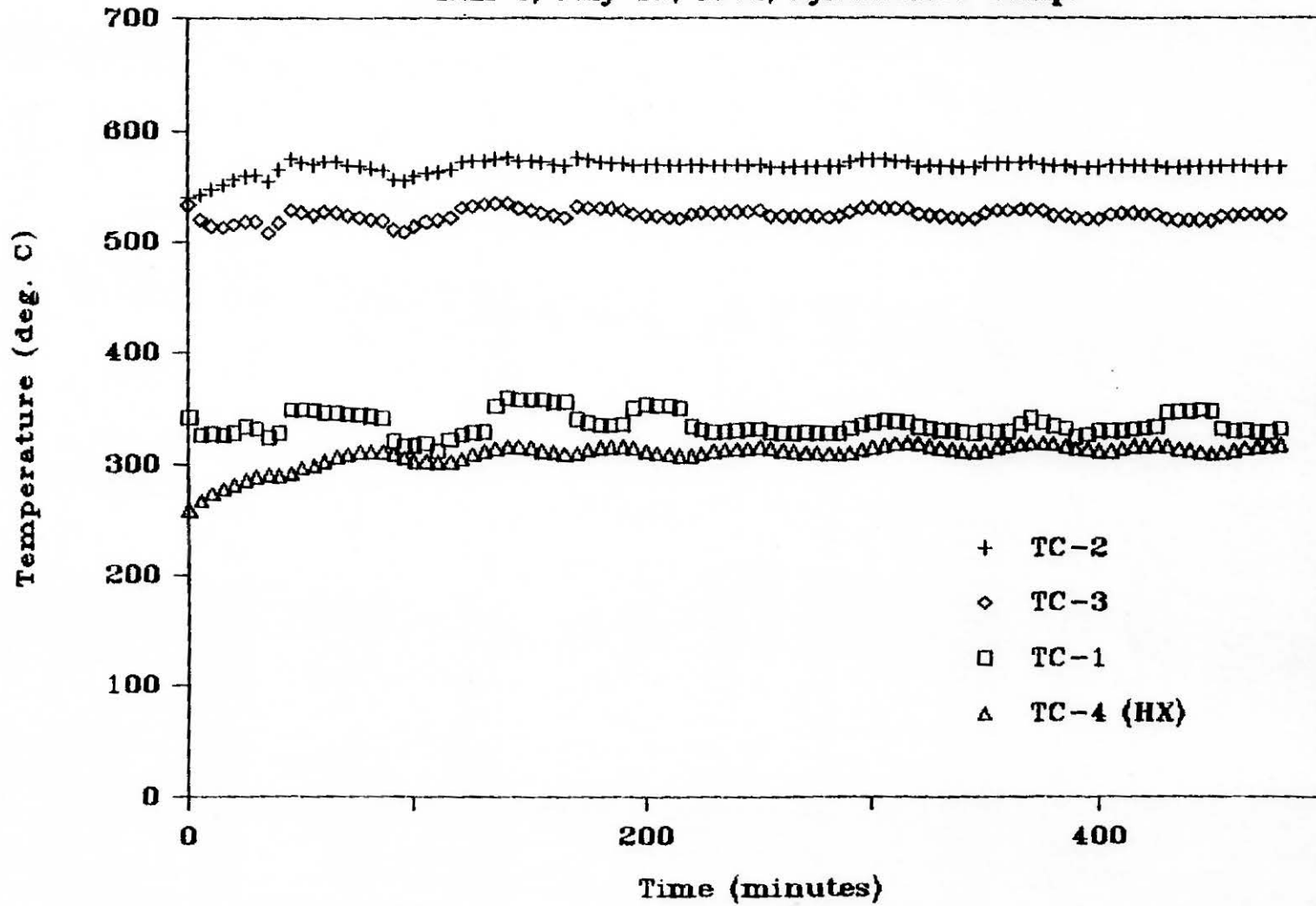


Fig. 27: Run #7 Dissociation Fractions

SANDIA SOLAR THERMAL

Run 8, July 10, 1984, Synthesizer Temp.



75

Fig. 29: Run #8 Synthesizer Temperatures

SANDIA SOLAR THERMAL

Run 9, July 11, 1984, Dissociator Temp.

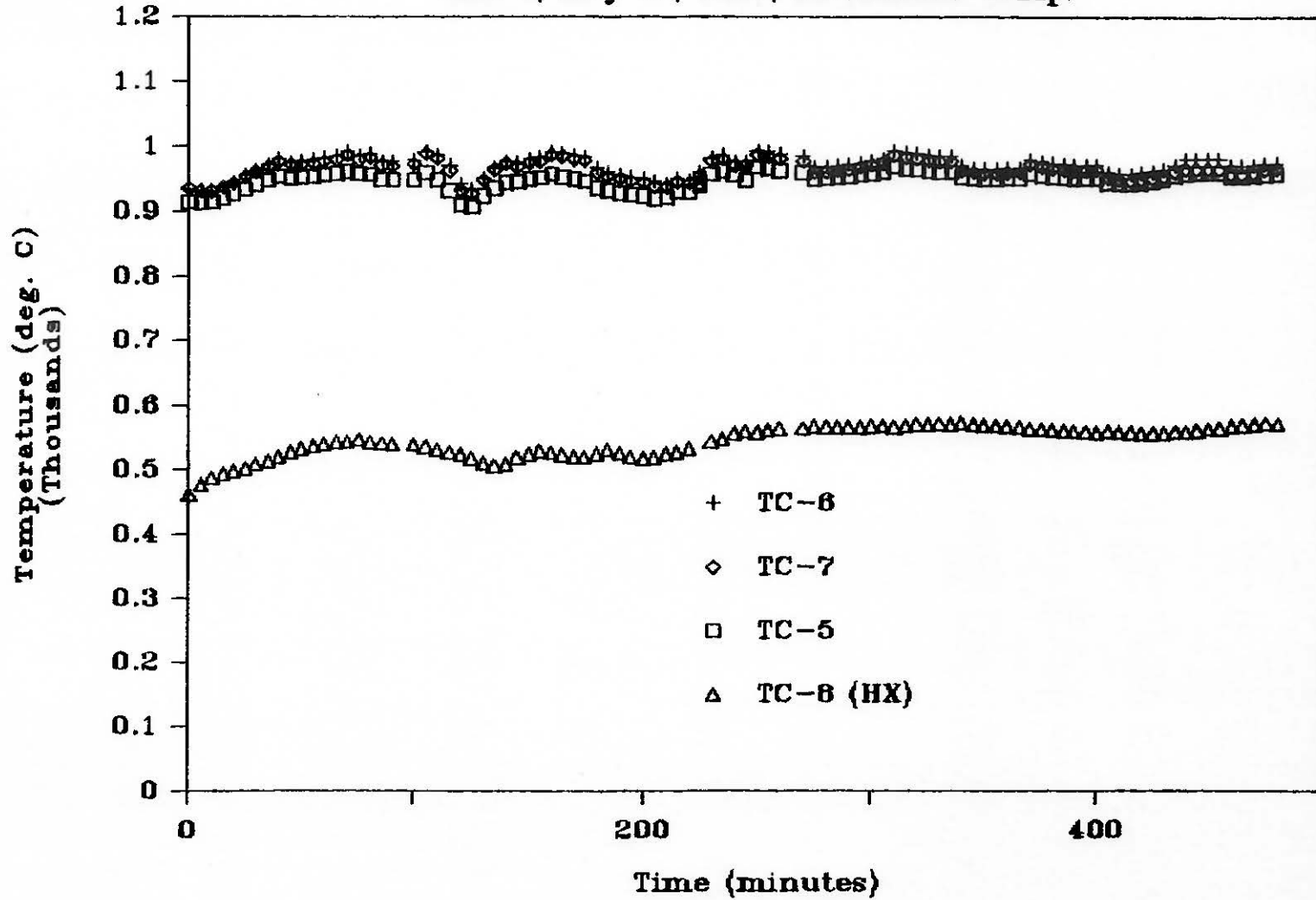


Fig. 31: Run #9 Dissociator Temperatures

SANDIA SOLAR THERMAL

Run 9, July 11, 1984, SO₂ Concentration

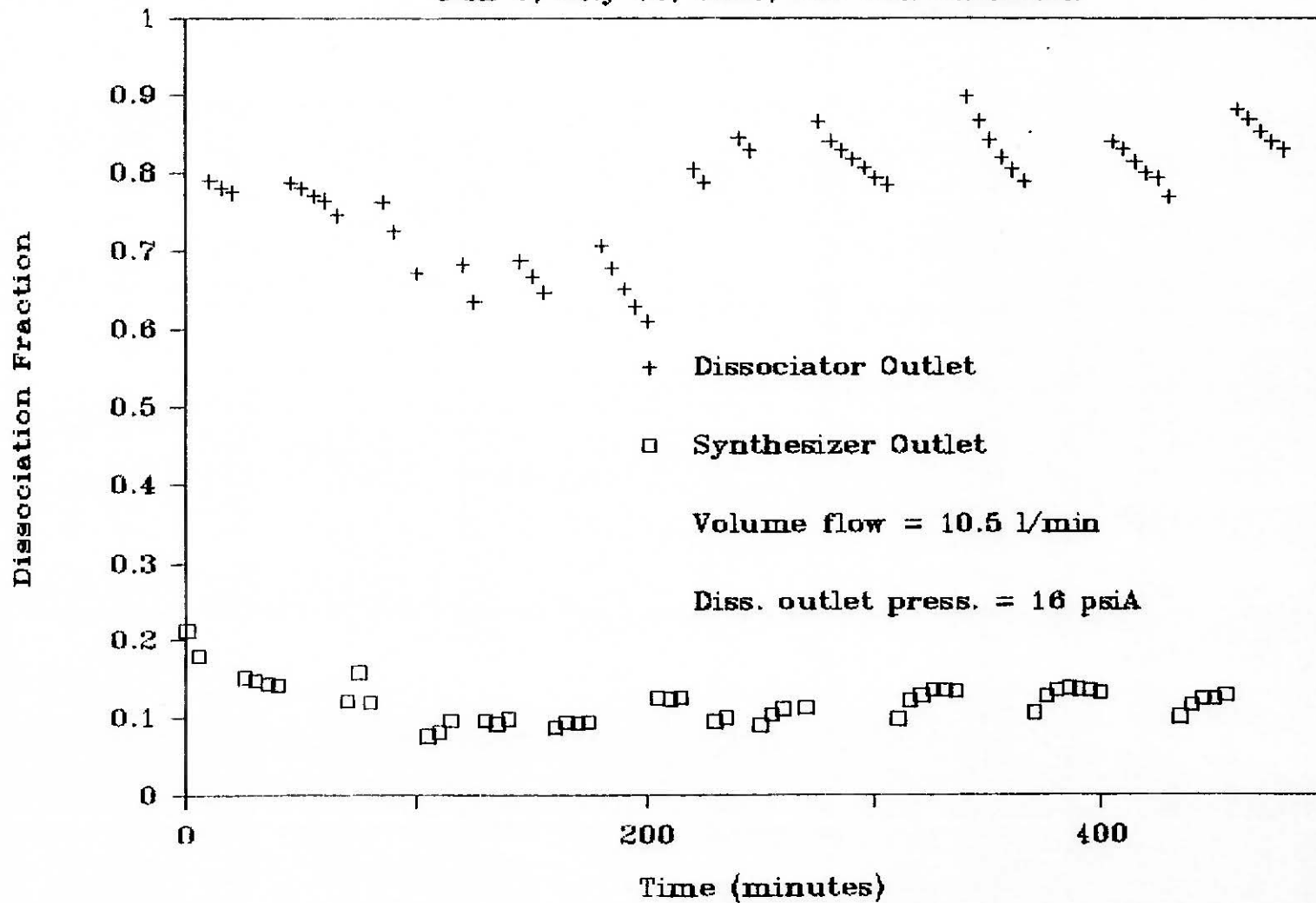


Fig. 33: Run #9 Dissociation Fractions

SANDIA SOLAR THERMAL

Run 10, July 12, 1984 Dissociator Temp.

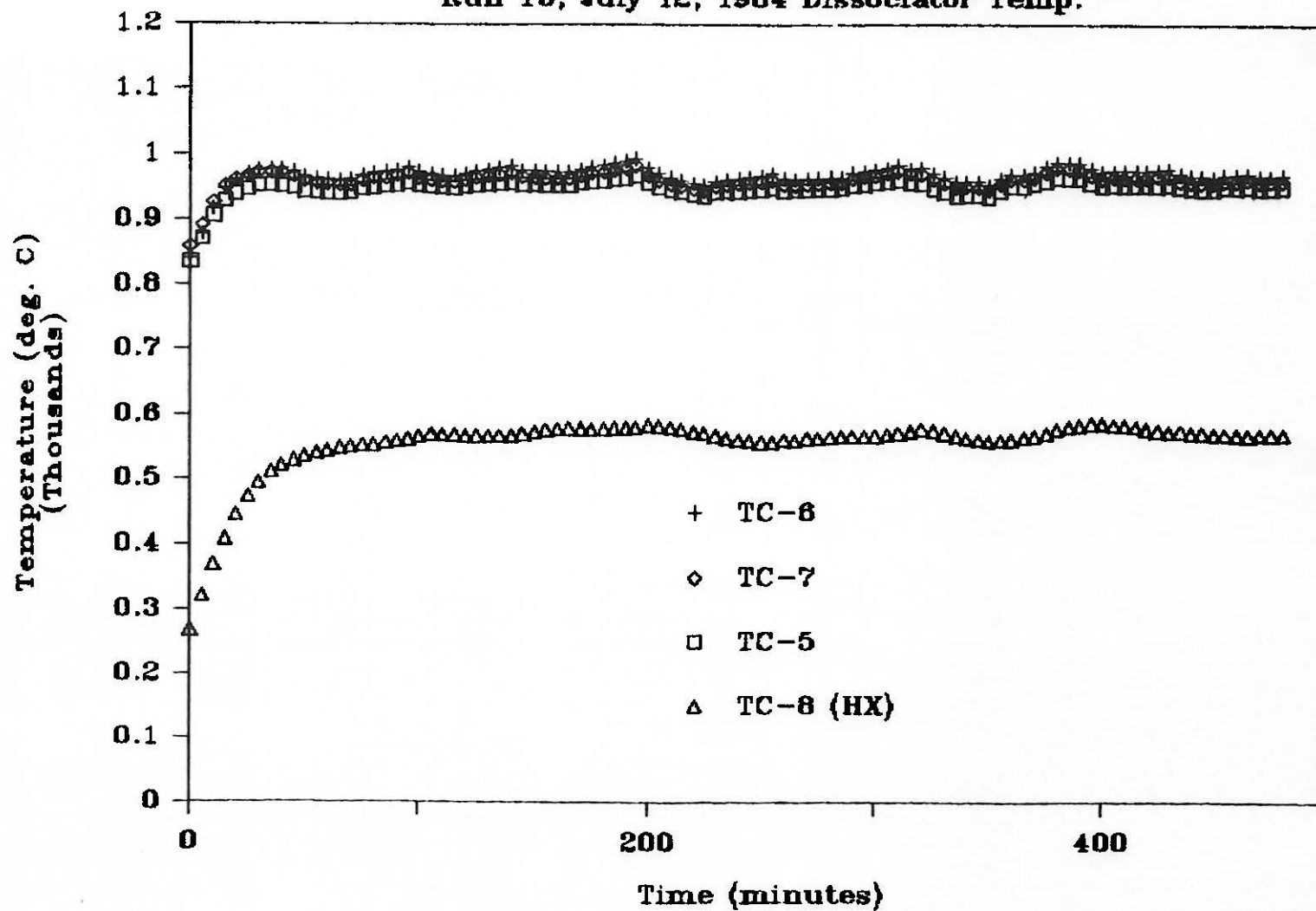


Fig. 34: Run #10 Dissociator Temperatures

SANDIA SOLAR THERMAL

Run 10, July 12, 1984 Synthesizer Temp.

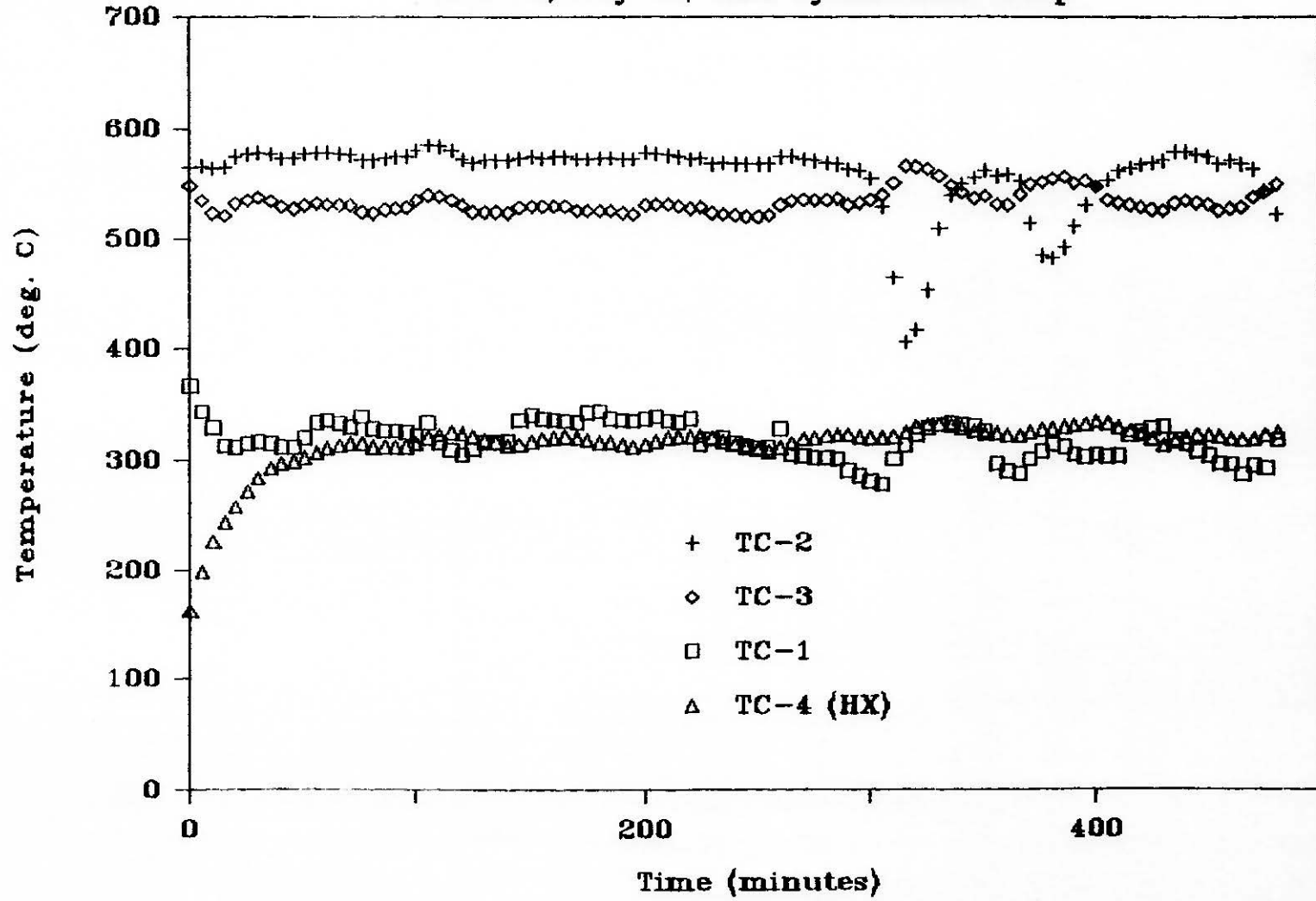


Fig. 35: Run #10 Synthesizer Temperatures

SANDIA SOLAR THERMAL

Run 10, July 12, SO₂ Concentration

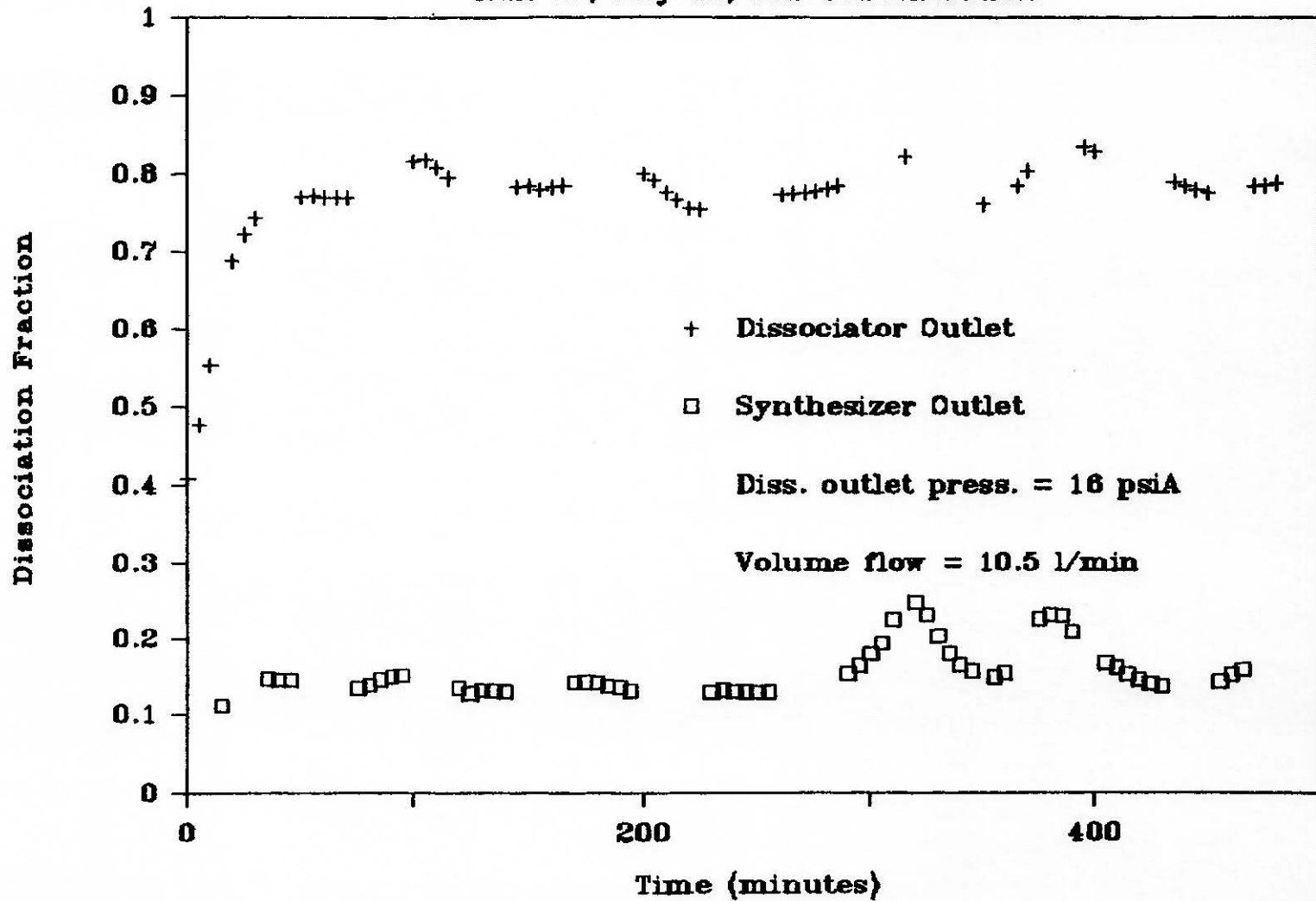


Fig. 36: Run #10 Dissociation Fractions

SANDIA SOLAR THERMAL

Run 11, July 13, 1984 Dissociator Temp.

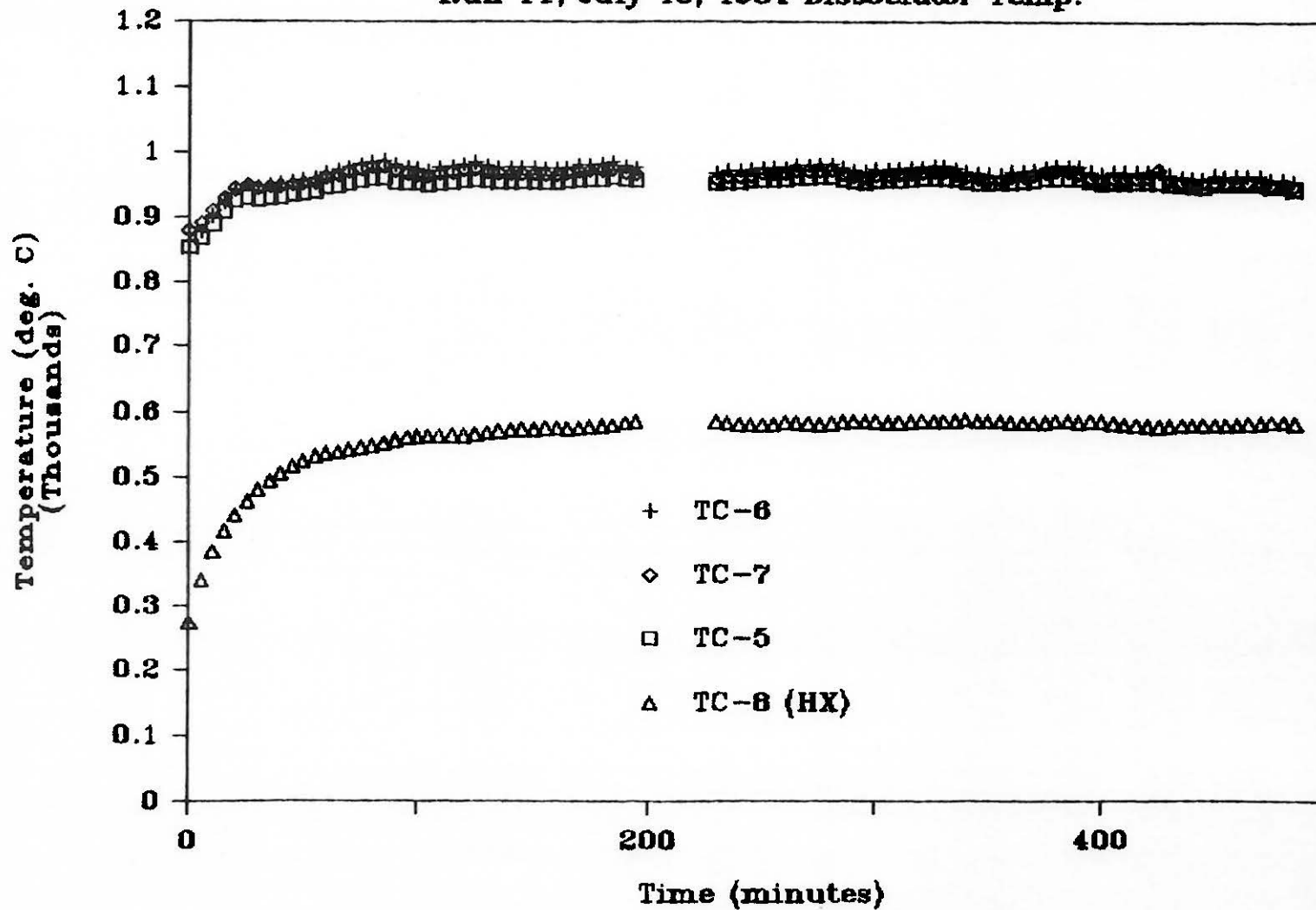
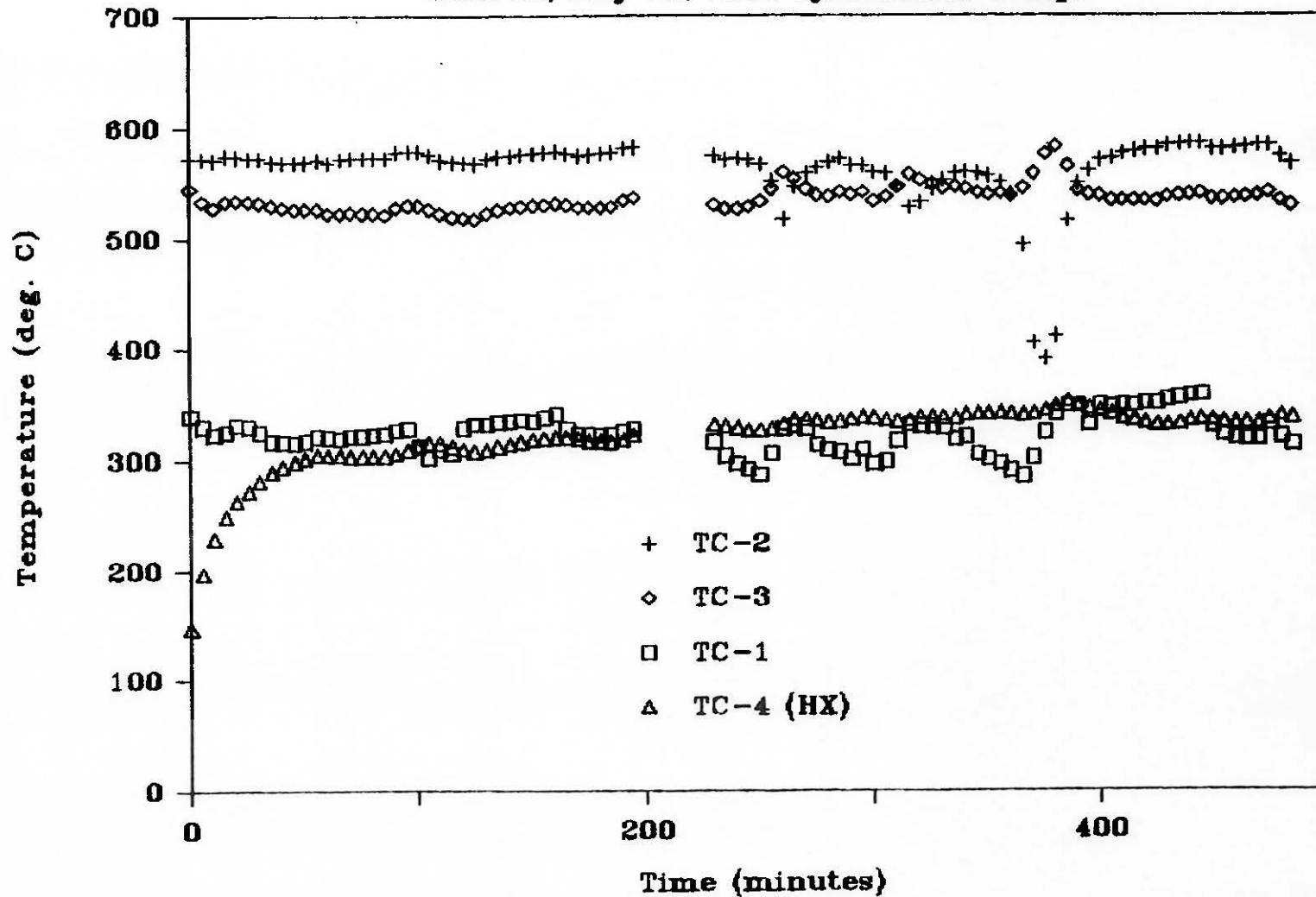


Fig. 37: Run #11 Dissociator Temperatures

SANDIA SOLAR THERMAL

Run 11, July 13, 1984 Synthesizer Temp.



84

Fig. 38: Run #11 Synthesizer Temperatures

SANDIA SOLAR THERMAL

Run 11, July 13, 1984 SO2 Concentration

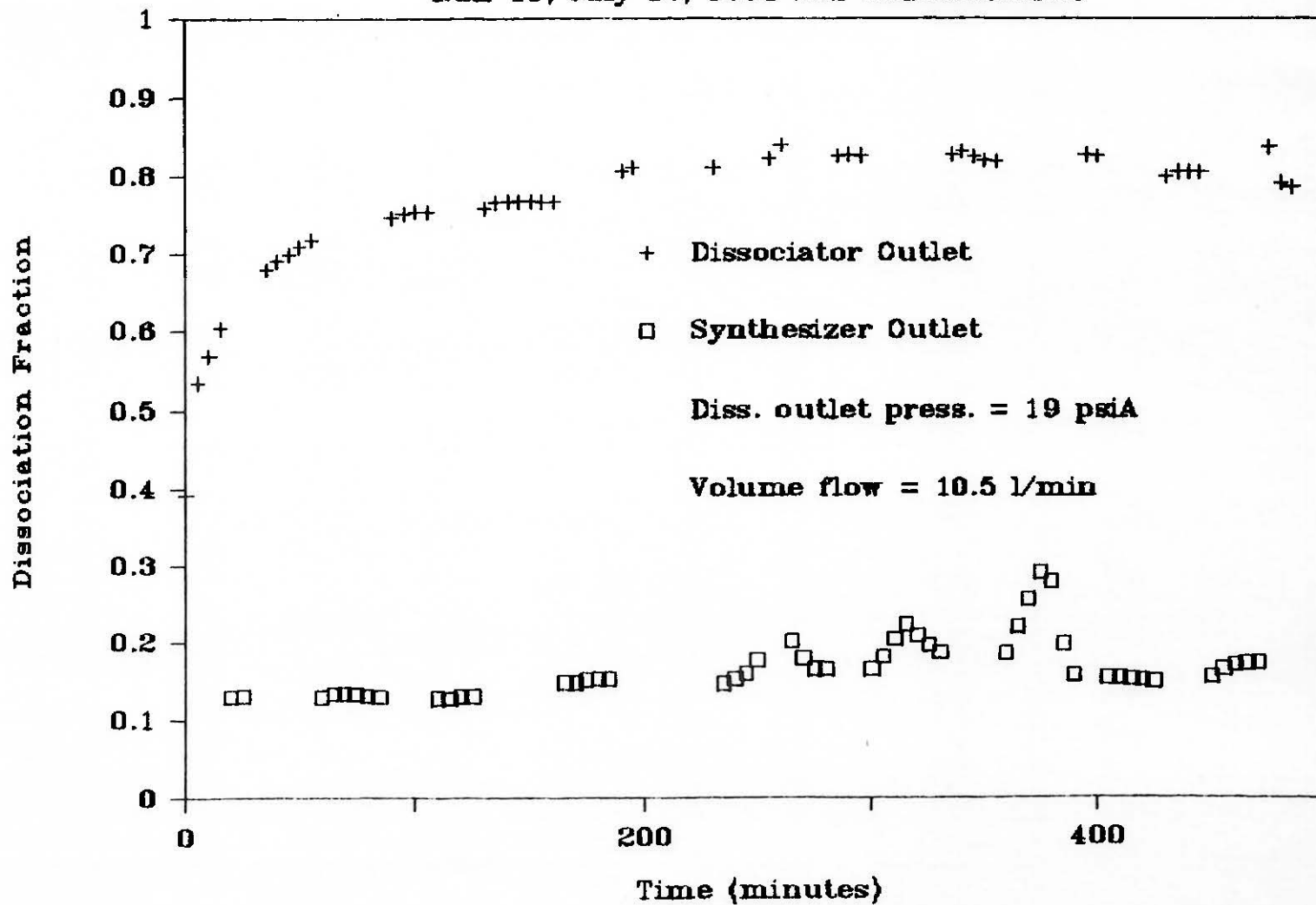


Fig. 39: Run #11 Dissociation Fractions

SANDIA SOLAR THERMAL

Run 12, Aug. 22, 1984, Dissociator Temp

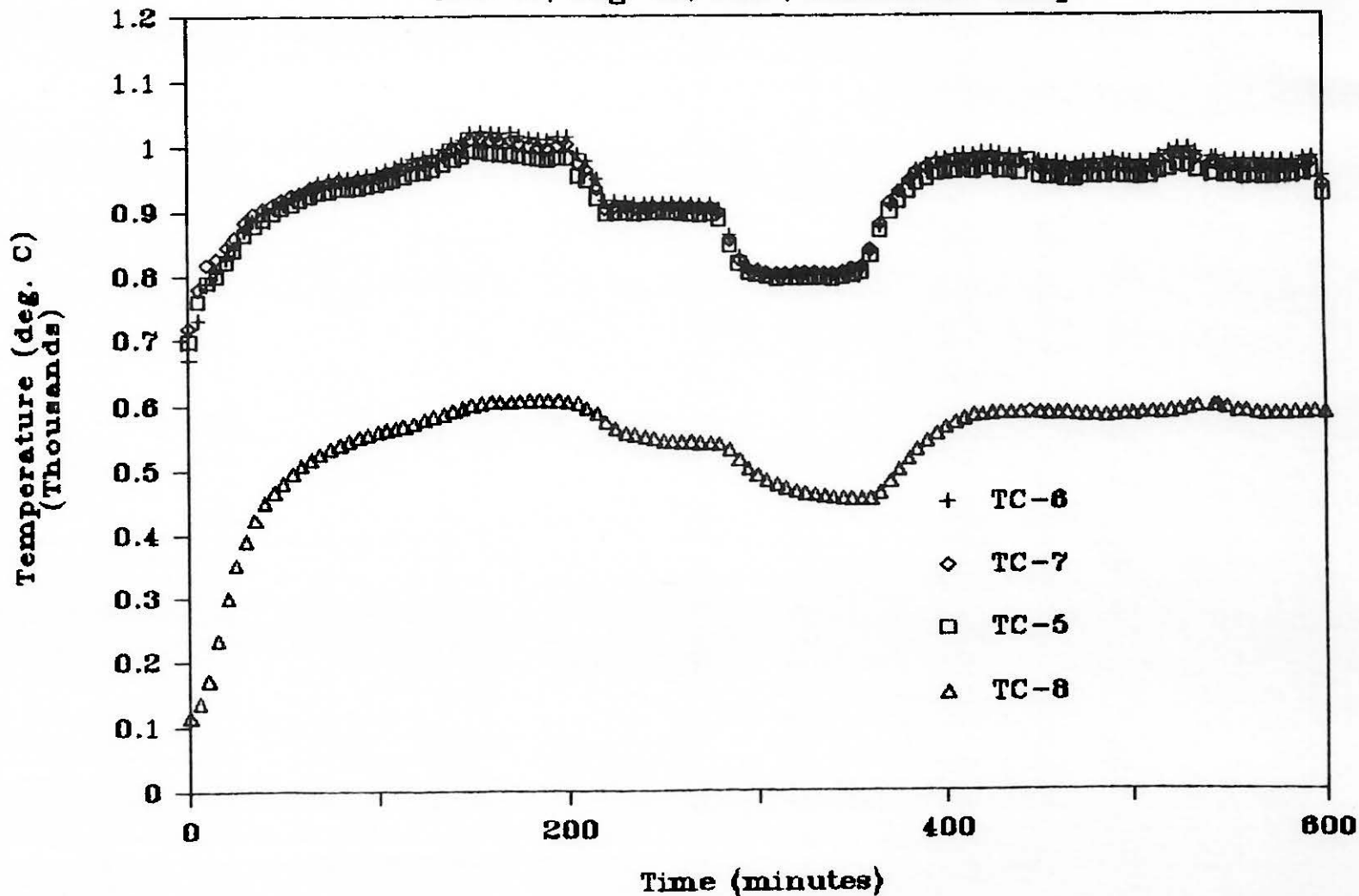
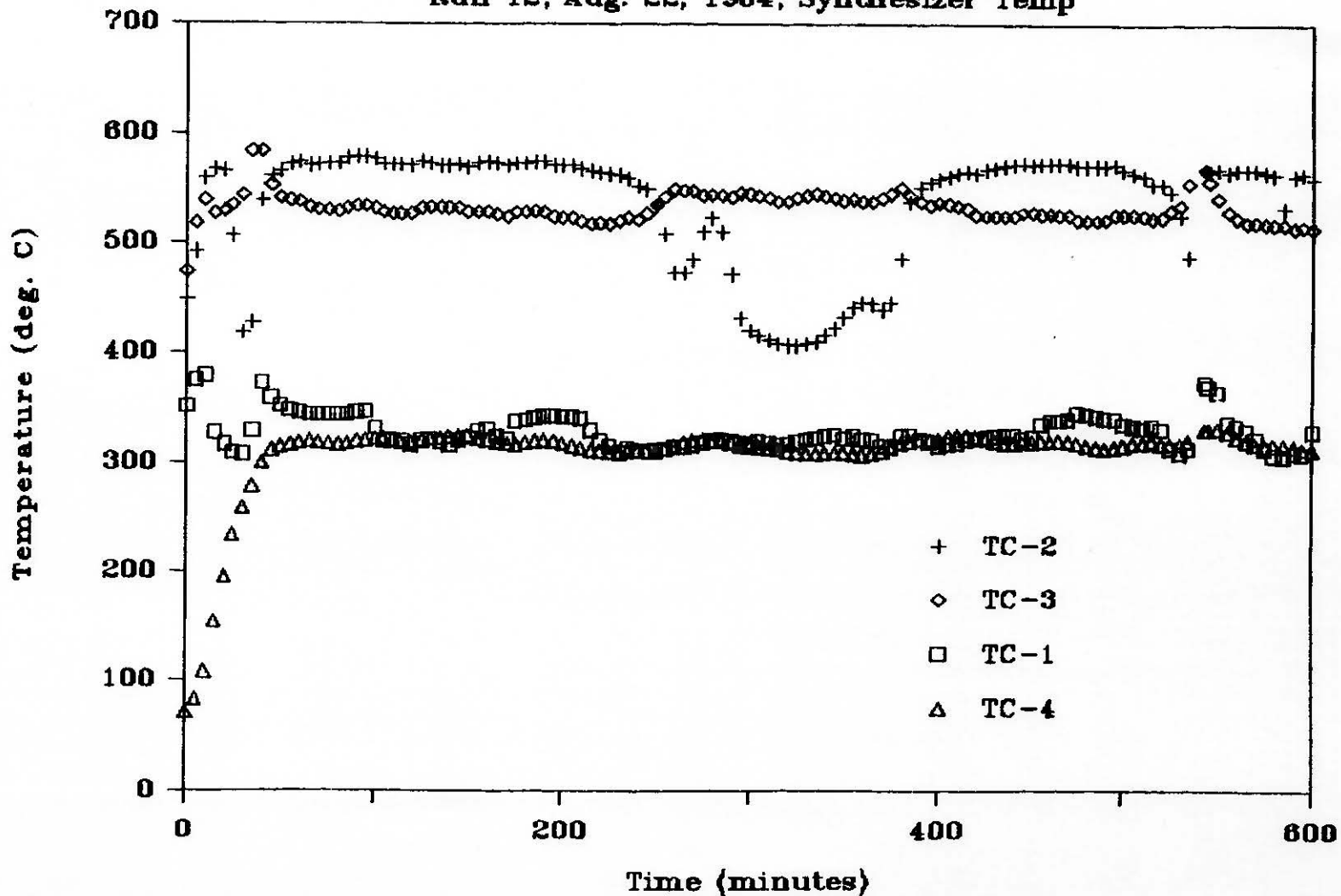


Fig. 40: Run #12 Dissociator Temperatures

SANDIA SOLAR THERMAL

Run 12, Aug. 22, 1984, Synthesizer Temp



87

Fig. 41: Run #12 Synthesizer Temperatures

SANDIA SOLAR THERMAL

Run 12, Aug 22, 1984, SO₂ Concentration

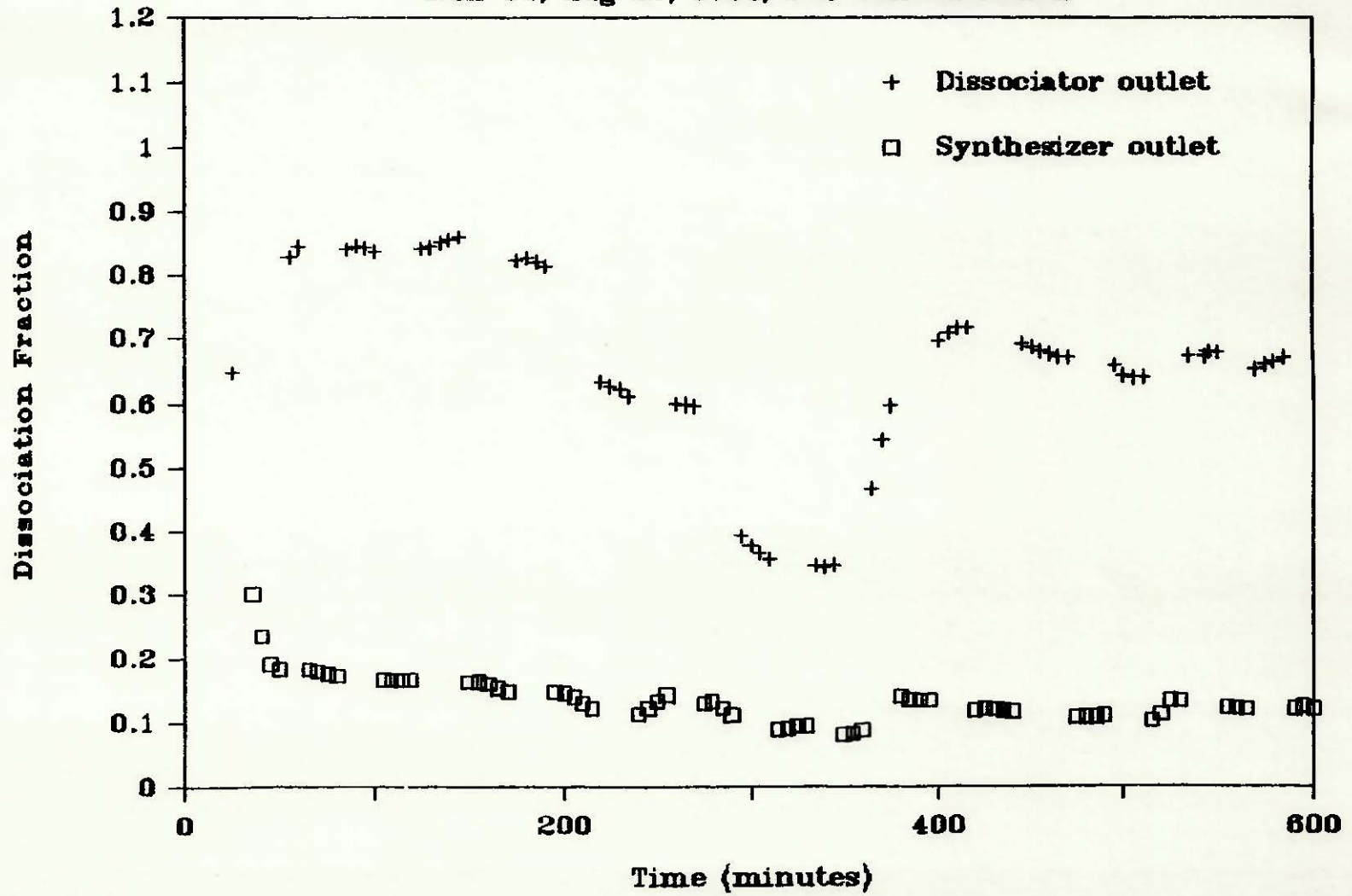


Fig. 42: Run #12 Dissociation Fractions

STANDARD DISTRIBUTION FOR SAND REPORTS (4/86)

DOE/TIC-4500(Rev.74)UC-62 (353)

AAI Corporation
P.O. Box 6787
Baltimore, MD 21204

Acurex Aerotherm (2)
555 Clyde Avenue
Mountain View, CA 94039
Attn: J. Schaefer
H. Morse

Alabama A&M University (2)
Department of Physics
P.O. Box 271
Normal, AL 35762
Attn: M. D. Aggarwal
A. Tan

Alpha Solarco
1014 Vine Street
Suite 2530
Cincinnati, OH 45202

Applied Concepts
405 Stoney Creek Blvd.
P.O. Box 490
Edinburg, VA 22824
Attn: J. S. Hauger

Applied Concepts
2501 S. Larimer County Rd. 21
Berthound, CO 80513
Attn: S. Pond

Australian National University
Department of Engineering Physics
P.O. Box 4
Canberra ACT 2600, AUSTRALIA
Attn: Prof. Stephen Kaneff

Barber-Nichols Engineering
6325 West 55th Ave.
Arvada, CO 80002
Attn: R. Barber

BDM Corporation
1801 Randolph Street
Albuquerque, NM 87106
Attn: W. E. Schwinkendorf

Battelle Memorial Institute
Pacific Northwest Laboratory
4000 NE 41st St.
Seattle, WA 98105
Attn: K. Drumheller

Battelle Memorial Institute
Pacific Northwest Laboratory
P.O. Box 999
Richland, WA 99352
Attn: T. Williams

Bechtel Group, Inc.
P.O. Box 3965
50 Beale Street
San Francisco, CA 94119
Attn: P. De Laquil

Black & Veatch
P.O. Box 8405
Kansas City, MO 64114
Attn: J. C. Grosskreutz

Boeing
Engineering & Construction
P.O. Box 3999
Seattle, WA 98124
Attn: R. Gillette

Budd Company (The)
Fort Washington, PA 19034
Attn: W. W. Dickhart

Budd Company (The)
Plastic R&D Center
356 Executive Drive
Troy, MI 48084
Attn: K. A. Iseler

Burns & Roe (2)
800 Kinderkamack Road
Oradell, NJ 07649
Attn: G. Fontana
R. Cherdack

Cal Poly State University
San Luis Obispo, CA 93407
Attn: E. J. Carnegie

California Institute of Technology Aeronautics Library MS 205-45 Pasadena, CA 91125 Attn: Jean Anderson	Electric Power Research Institute 3412 Hillview Avenue Palo Alto, CA 94303 Attn: E. A. Demeo J. E. Cummings
California Polytechnic University Dept. of Mechanical Engineering Pamona, CA 91768 Attn: W. B. Stine	Energy Technology Engr. Ctr. Rockwell International Corp. P.O. Box 1449 Canoga Park, CA 91304 Attn: W. L. Bigelow
Chicago Bridge and Iron 800 Jorie Blvd. Oak Brook, IL 60521 Attn: J. M. Shah	ENTECH, Inc. P.O. Box 612246 DFW Airport, TX 75261 Attn: R. R. Walters
Colorado State University Ft. Collins, CO 80523 Attn: T. G. Lenz	Eurodrive, Inc. 30599 San Antonio Rd. Hayward, CA 94544
Columbia Gas System Service Corp. 1600 Dublin Road Columbus, OH 43215 Attn: J. Philip Dechow	Florida Solar Energy Center 300 State Road 401 Cape Canaveral, FL 32920 Attn: Library
Custom Engineering, Inc. 2805 South Tejon Street Englewood, CO 80110 Attn: C. Demoraes	Ford Aerospace Ford Road Newport Beach, CA 92663 Attn: R. H. Babbe
Datron Systems, Inc. 200 West Los Angeles Ave. Simi Valley, CA 93065-1650	Ford Motor Company Glass Div., Technical Center 25500 West Outer Drive Lincoln Park, MI 48246 Attn: V. L. Lindberg
DSET Box 1850 Black Canyon Stage I Phoenix, AZ 85029 Attn: G. A. Zerlaut	Foster Wheeler Solar Dev. Corp. 12 Peach Tree Hill Road Livingston, NJ 07039 Attn: M. D. Garber
Donnelly Corporation 49 West Third Street Holland, MI 49423 Attn: M. DeVries	Georgia Power Co. 7 Solar Circle Shenandoah, GA 30264 Attn: E. Ney
Dow Chemical Company Contract Research, Development, and Engr. Building 566 Midland, MI 48640 Attn: J. F. Mulloy	Heery Energy Consultants, Inc. Project Energy Manager 880 West Peachtree St. NW Atlanta, GA 30309 Attn: Glenn Bellamy
Dow Corning Corporation Midland, MI 48640 Attn: G. A. Lane	

Highland Plating
10001 N. Orange Drive
Los Angeles, CA 90038
Attn: D. May

Industrial Solar Technologies
5775 West 52nd Ave.
Denver, CO 80212
Attn: Randy Gee

Institute of Gas Technology
Attn: Library
34245 State Street
Chicago, IL 60616

Jet Propulsion Laboratory
4800 Oak Grove Drive
Pasadena, CA 91109
Attn: M. Alper

Kearney & Associates
14022 Condessa Drive
Del Mar, CA 92014
Attn: David W. Kearney

LaCour Kiln Service
P.O. Box 247
Canton, MS 39046
Attn: J. A. LaCour

LaJet Energy Co.
P.O. Box 3599
Abilene, TX 79604
Attn: Monte McGlaun
Carl Williams

L'Garde, Inc.
1555 Placentia Avenue
Newport Beach, CA 92663
Attn: Mitchell Thomas

John Lucas
865 Canterbury Road
San Marino, CA 91108

Martin Marietta Corp.
P.O. Box 179
Denver, CO 80201
Attn: T. Tracy

McCarter Corporation
200 E. Washington St.
P.O. Box 351
Norristown, PA 19404
Attn: R. A. Powell

McDonnell-Douglas Astronautics
Company (3)
5301 Bolsa Avenue
Huntington Beach, CA 92647
Attn: J. B. Blackmon
J. Rogan
D. Steinmeyer

Mechanical Technology, Inc. (2)
968 Albany Shaker Road
Latham, NY 12110
Attn: G. R. Dochat
J. Wagner

Meridian Corporation
5113 Leesburg Pike
Suite 700
Falls Church, VA 22041
Attn: D. Kumar

Midwest Research Institute (2)
425 Volker Blvd.
Kansas City, MO 64110
Attn: R. L. Martin
J. Williamson

NASA Lewis Research Center (2)
21000 Brook Park Road
Cleveland, OH 44135
Attn: R. Beremand 500-215
R. C. Evans 500-210

Naval Civil Engr. Laboratory
Port Hueneme Naval Station
Port Hueneme, CA 93043
Attn: Louis Huang

New Mexico Solar Energy Institute
New Mexico State University
Box 3SOL
Las Cruces, NM 88003

Parsons of California
3437 S. Airport Way
Stockton, CA 95206
Attn: D. R. Biddle

PG&E
3400 Crow Canyon Rd.
San Ramon, CA 94583
Attn: J. Iannucci
G. Braun

Power Kinetics, Inc.
1223 Peoples Avenue
Troy, NY 12180
Attn: W. E. Rogers

Reinhold Industries
Division of Keene Corp.
1287 E. Imperial Highway
Santa Fe Springs, CA 90670
Attn: J. Flynt

Research Systems, Inc.
Suburban Trust Bldg.,
Suite 203
5410 Indian Head Hwy.
Oxon Hill, MD 20745
Attn: T. A. Chubb

Rockwell International
Energy Systems Group
8900 De Soto Avenue
Canoga Park, Ca 91304
Attn: T. Springer

Rockwell International
Space Station Systems Division
12214 Lakewood Blvd.
Downey, CA 90241
Attn: I. M. Chen

Sanders Associates
MER 15-2350
C.S. 2035
Nashua, NH 03061-2035
Attn: B. Davis

Science Applications
International Corp.
10401 Roselle Street
San Diego, CA 92121
Attn: Barry Butler

Solar Energy Research Inst. (6)
1617 Cole Blvd.
Golden, CO. 80401
Attn: G. Gross
B. P. Gupta
J. Thornton
D. Johnson
M. Murphy
D. Hawkins

Solar Kinetics, Inc.
P.O. Box 47045
Dallas, TX 75247
Attn: J. A. Hutchison

Solar Steam
Suite 400
Old City Hall
625 Commerce Street
Tacoma, WA 98402
Attn: D. E. Wood

SLEMCO
19655 Redberry Dr.
Los Gatos, CA 95030
Attn: A. J. Slemmons

Stearns-Catalytic Corp.
Box 5888
Denver, CO 80217
Attn: W. R. Lang

Sun Exploration and Production Co.
P.O. Box 2880
Dallas, TX 75221-2880
Attn: R. I. Benner

Sun Power, Inc.
6 Byard St.
Athens, OH 45701
Attn: Mac Thayer

Sundstrand ATG (2)
P.O. Box 7002
Rockford, IL 61125
Attn: A. W. Adam
B. G. Johnson

Suntec Systems, Inc.
P.O. Box 315
Savage, MN 55378
Attn: Harrison Randolph
J. H. Davison

Swedlow, Inc.
12122 Western Avenue
Garden Grove, CA 92645
Attn: E. Nixon

3M-Energy Control Products (2)
207-1W 3M Center
St. Paul, MN 55144
Attn: B. Benson
J. L. Roche

Texas Tech University
Dept. of Electrical Engineering
P.O. Box 4439
Lubbock, TX 79409
Attn: E. A. O'Hair

TRW (3)
Space & Technology Group
One Space Park
Redondo Beach, CA 90278
Attn: G. M. Reppucci
A. D. Schoenfeld
J. S. Archer

U.S. Department of Energy (4)
Albuquerque Operations Office
P.O. Box 5400
Albuquerque, NM 87185
Attn: D. Graves
R. Y. Lowrey
J. Weisiger
N. Lackey

U.S. Department of Energy
Office of Solar Heat Technologies
Forrestal Building
Washington, DC 20585
Attn: Fred Morse

U.S. Department of Energy
Office of Solar Heat Technologies
Forrestal Building
Washington, DC 20585
Attn: C. Carwile

U.S. Department of Energy
Division of Solar Thermal Tech.
Forrestal Building
Washington, DC 20585
Attn: Howard S. Coleman
R. Shivers
S. Gronich
C. Mangold
M. Scheve
F. Wilkins

US Department of Energy
San Francisco Operations Ofc.
1333 Broadway
Oakland, CA 94612
Attn: R. W. Hughey

University of Houston
Energy Laboratory; SPA
Houston, TX 77004
Attn: Lorin Vant-Hull

University of Kansas
Center for Research
2291 Irving Hill Dr.
Lawrence, KA 66045
Attn: David Martin

University of New Mexico (2)
Department of Mechanical Engr.
Albuquerque, NM 87131
Attn: M. W. Wilden
W. A. Gross

USS Chemicals
P.O. Box 127
Ironton, OH 45638
Attn: E. H. Weber

Viking Solar Systems, Inc.
3223 N. Verdugo Rd.
Glendale, CA 91208
Attn: George Goranson

0400 R. P. Stromberg
1510 J. W. Nunziato
1513 D. W. Larson
1810 R. G. Kepler
1820 R. E. Whan
1824 J. N. Sweet
1830 M. J. Davis
1832 W. B. Jones
1840 R. J. Eagan
1841 R. B. Diegle
1842 R. E. Loehman
1846 D. H. Doughty
2520 N. J. Magnani
2525 R. P. Clark
2540 G. N. Beeler
2541 J. P. Abbin
3141 S. A. Landenberger (5)
3151 W. L. Garner (3)
3154 C. H. Dalin (28) for DOE/OSTI
3160 J. E. Mitchell
6200 V. L. Dugan
6220 D. G. Schueler
6221 E. C. Roes
6222 J. V. Olts
6223 G. J. Jones
6224 D. E. Arvizu

6227 J. I. Martinez (10)
6225 H. M. Dodd
6226 J. T. Holmes
6227 J. A. Leonard (20)
6228 P. J. Eicker
6250 B. W. Marshall
6254 B. Granoff
8024 P. W. Dean
8470 R. L. Rinne
8471 A. C. Skinrood